

COURSE 6

Matching Rules and Quasiperiodicity: the Octagonal Tilings

A. Katz

*Centre de Physique Théorique, Ecole Polytechnique
91128 Palaiseau Cedex
France*

1. INTRODUCTION

This lecture discusses one of the most important question raised by the discovery of quasicrystals: the onset of quasiperiodic order. In fact, one of the main problems about quasicrystals is to understand the simple possibility of a non periodic long range order, since no two atoms have exactly the same environment up to infinity. One possible solution to this problem is to consider that the order stems from privileged local configurations and is able to propagate throughout the structure. This point of view deals with the existence of local constraints which would enforce the quasiperiodic order: these are the so-called “local rules”, or “matching rules” in tiling language.

Although the atomic structure of quasicrystals is not linked with quasiperiodic tilings in the same strong way that crystals are linked with periodic tilings, it makes sense to approach the problem of ordering of quasicrystals through the simpler and schematic theory of matching rules for tilings. The reason is that experiments suggest that real quasicrystals share a main geometrical property with the kind of “canonical tilings” which will be studied here: within experimental resolution, it seems that there is only a *finite* number of different atomic environments (up to a given distance) for atoms in the quasicrystal. This “rigidity” feature, which is described by the “flatness” of the atomic surfaces to be defined below, obviously occurs also for tilings, so that the notion of matching

rules for tilings, which prescribes how the tiles should be joined together, is not so far from the notion of local rules (L. Levitov [1]) which prescribes for a quasicrystal what are the allowed local neighbourhoods of atoms.

In other words, we shall consider here quasiperiodic tilings as abstract patterns carrying the long range order typical of the atomic structures of quasicrystals.

Thus, from now on, we shall deal only with tilings. For the sake of simplicity, we shall develop our arguments for two-dimensional tilings, and even more specifically in the case of the octagonal and related tilings. But, as will be made clear, the approaches explained in this lecture are by no means limited to the two-dimensional case.

Let us now define more precisely this notion of matching rules. For tilings, they consist in decorations (typically, arrowing of the edges of the tiles for a two-dimensional tiling) together with a “recipe” which prescribes how the decorations of adjacent tiles should fit with each other [1][2][3][4]. We say that a tiling admits matching rules when such a set of *local* constraints enforces the quasiperiodicity of the tiling (a *global* property) as soon as they are satisfied everywhere in the tiling of the whole space.

The very existence of such rules is by no means obvious. Matching rules for the original Penrose tilings were derived in several forms by Roger Penrose using the self-similarity (inflation and deflation) of his tilings. For the sake of completeness and reference purpose, we shall give a short account of this approach, referring for instance to the paper [3] by F. Gähler for more details about what he called the composition-decomposition method (the author thanks F. Gähler for his help in the redaction of this section). The remainder of the paper is devoted to a quite different approach initiated by the author in [2] and developed subsequently in collaboration with L. Levitov.

2. QUASIPERIODIC TILINGS

We will focus our attention on the best known class of quasiperiodic systems, which are the canonical or “Penrose-like” tilings. They are named after Roger Penrose, who discovered a strikingly simple non-periodic tiling of the plane with five-fold symmetry [5] later studied in detail by N. G. de Bruijn [6]. Although the original construction relied mainly on self-similarity properties (see section 3.1) and the quasiperiodicity of the tilings was recognised only later by crystallographers and solid state physicists, these tilings are in fact the simplest non-trivial quasiperiodic sets of points that one can imagine.

2.1. Quasiperiodicity

Let us first recall briefly the definition of quasiperiodicity, as developed by H. Bohr [7][8][9] and A. S. Besicovic [10]: a function (of d real variables) on an affine (d -dimensional) space \mathbf{E}_c is said to be *quasiperiodic* if it is the restriction

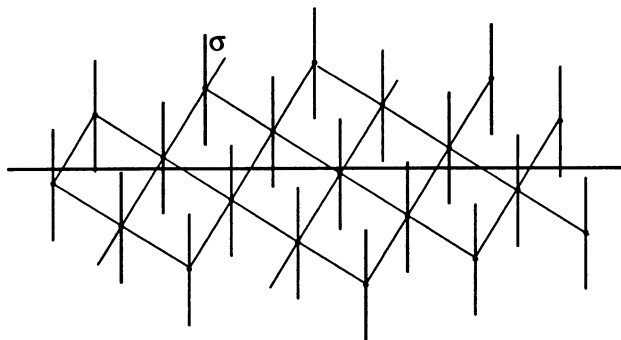


Fig. 1. — Atomic surfaces in the 2 dimensional case; the cut space E_c is the horizontal line; the atomic surfaces σ are line segments transversal to E_c and attached at the lattice nodes of Λ .

to E_c (embedded as an affine subspace) of a periodic function of n real variables defined in a higher-dimensional space \mathbb{R}^n . Of course, if the embedded space E_c (which will be referred to as the “cut”) is rationally oriented with respect to the lattice of periods of the periodic function (i. e., if E_c is parallel to a lattice subspace) then the restriction of this function to E_c is also periodic. But if the direction of the cut is irrational, that is, if the vector subspace parallel to the cut contains no point of the lattice besides the origin, then the restriction is not a periodic function, but a strictly quasiperiodic one.

2.2. The Atomic Surfaces

To describe a quasiperiodic set of points rather than a quasiperiodic function, the natural generalisation is to attach to each of these points a Dirac delta and to consider them as the d -dimensional restriction μ of a n -dimensional periodic measure, say $\tilde{\eta}$, instead of the restriction of a periodic (smooth) function. Let Λ be the lattice of periods of this periodic measure. The carrier of $\tilde{\eta}$ defines a Λ -periodic geometric locus $\tilde{\sigma}$ which decomposes, in the elementary domains, into identical pieces σ . The manifold σ is called the “atomic surface” and $\tilde{\sigma}$ is the periodic set of atomic surfaces as shown on Fig. 1.

The intersections between the cut and the atomic surfaces, and therefore the resulting structure, are well defined each time the cut is transversal to the atomic surfaces. The transversality condition means that the cut does not intersect any atomic surface on its boundary or on a point where the tangent space to the atomic surface is parallel to the cut. This is not a strong restriction; it simply means, in a first approach, that the atomic surface boundaries are not a too complicated set, such as for example, a fractal set. Observe that since the cut E_c is of dimension d and the boundaries of the atomic surfaces are (piece-wise smooth) submanifolds of dimension $(n - d - 1)$ or less, their non-

intersection is a generic property in \mathbb{R}^n , which means that almost all choices of \mathbf{E}_c will work.

2.3. The cut algorithm

To generate the quasiperiodic set of points, we simply collect the intersection points of $\tilde{\sigma}$ with \mathbf{E}_c . We designate by \mathbf{E}_{\parallel} the vector subspace of \mathbb{R}^n defining the direction of the cut \mathbf{E}_c and by \mathbf{E}_{\perp} the perpendicular subspace. This algorithm is nothing but a slight generalisation (first advocated by P. Bak [11]) of the former “hyperspace” formalism developed by Janner and Janssen [12] from the pioneer work of de Wolff [13] for modulated and incommensurate structures.

For a given generic direction of the cut, the technique requires an additional set of parameters which specifies the relative location of the cut space \mathbf{E}_c with respect to Λ . Indeed, one generates infinitely many “different” quasiperiodic set of points by shifting the cut space: observe that for a generic atomic surface, two parallel cuts yield isometric structures if and only if they are mapped on each other by a translation belonging to the lattice, up to a translation parallel to the cut. Such a translation is a vector in \mathbb{R}^n which projects on the subspace orthogonal to the direction of the cut, on a vector belonging to the projection of the lattice. Thus we see that the different structures are classified by the quotient of this subspace by the projection of the lattice. Since this last set is countable, we see that by shifting the cut we generate an uncountable infinity of different (non-isometric) structures.

2.4. Canonical or “Penrose like” tilings

2.4.1. Definition

Let us start with the general definition of what we call tilings of the Penrose type [14] or canonical tilings: they are obtained by the cut method with one atomic surface σ per unit cell defined by the projection on \mathbf{E}_{\perp} along \mathbf{E}_{\parallel} of the unit cell γ_n of Λ . To construct a d -dimensional canonical tiling, consider in \mathbb{R}^n the simple cubic lattice \mathbf{Z}^n generated by the canonical orthonormal basis of \mathbb{R}^n , which spans the unit cube γ_n . Then choose any d -dimensional subspace \mathbf{E}_{\parallel} in \mathbb{R}^n , and denote by \mathbf{E}_{\perp} the orthogonal subspace. We define the atomic surface σ by projecting orthogonally γ_n on \mathbf{E}_{\perp} . This yields a $(n - d)$ -dimensional polyhedron, and the corresponding lattice $\tilde{\sigma}$ of atomic surfaces in \mathbb{R}^n is obtained by copying this polyhedron at each vertex ξ of \mathbf{Z}^n .

The vertices of our tilings are the intersections of $\tilde{\sigma}$ with any d -dimensional plane cut \mathbf{E}_c parallel to \mathbf{E}_{\parallel} , and which is everywhere transversal to $\tilde{\sigma}$, i.e., which does not intersect any of the boundaries $\partial\sigma_{\xi}$ for $\xi \in \mathbf{Z}^n$.

The simplest example of this construction is obtained with $n = 2$ and $d = 1$, and is depicted on Fig. 1. For an irrationally oriented \mathbf{E}_{\parallel} , we get a quasiperiodic tiling of the cut \mathbf{E}_c by means of two segments, which are the projections of the two edges of the unit square γ_2 . Although this construction may look rather trivial, it deserves attention because the most important features of this class of

tilings already appear in this simple case and may be discussed in a dimension-independent way.

2.4.2. The oblique tiling

To prove that we actually get a tiling by means of the projections of the edges of the square, the best way is to construct the so-called *oblique tiling* [15] or *Klötze decomposition* [16].

The idea is the following: consider any tiling of \mathbb{R}^n and any plane cut through this tiling. Each time the cut is generic, that is, intersects transversally the boundaries of the tiles, the traces of the tiles on the cut make up a covering of the cut, without overlappings or holes. But this covering is not a tiling in general, since there is no reason for the traces of the tiles to belong to a finite set of shapes. For instance, consider a cut \mathbf{E}_c with an irrational slope through the standard square tiling of the plane: since there is no minimal distance between the vertices of the tiling and the cut, there is no minimal length for the segments of the induced covering of the cut, and this entails that there are infinitely many different lengths in this covering, which therefore is not a tiling.

However, it is possible to adapt the shape of the tiles of a periodic tiling of \mathbb{R}^n to the direction of the cut, in order to obtain only a *finite* number of shapes in the generic cuts: the trick is to make the boundaries of the tiles parallel to either the direction of the cut \mathbf{E}_{\parallel} or to the orthogonal subspace \mathbf{E}_{\perp} . For our low dimensional case, the construction of this oblique tiling is the following:

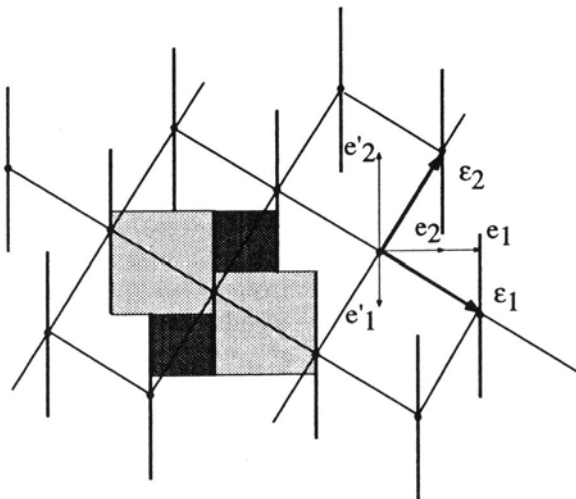


Fig. 2. — Construction of the oblique tiling for the linear quasiperiodic chain. The “oblique tiles” are the sum of a (horizontal) tile of the quasiperiodic chain and of its so-called “existence domain” (here a vertical segment)

let us start with the unit square, spanned by the canonical basis $(\varepsilon_1, \varepsilon_2)$ of \mathbb{R}^2 . Defining π_{\parallel} (resp. π_{\perp}) as the orthogonal projection on \mathbf{E}_{\parallel} (resp. \mathbf{E}_{\perp}), we set $e_i = \pi_{\parallel}(\varepsilon_i)$ and $e'_i = \pi_{\perp}(\varepsilon_i)$ ($i = 1, 2$), in such a way that $\varepsilon_i = e_i + e'_i$. Let us distort the edge ε_1 along the broken line defined by the segment e'_1 followed by the segment e_1 . We see that the union $\{e'_1, \varepsilon_2\} \cup (e'_1 + \{e_1, \varepsilon_2\})$ of the two parallelograms spanned by $\{e_1, \varepsilon_2\}$ and $\{e'_1, \varepsilon_2\}$ is still a unit cell for the lattice \mathbb{Z}^2 . Now, let us proceed to the same decomposition for the vector ε_2 and each parallelogram: we get a new unit cell of \mathbb{Z}^2 made of four subcells spanned by $\{e'_1, \varepsilon_2\}$, $\{e'_1, e'_2\}$, $\{e_1, \varepsilon_2\}$ and $\{e_1, e'_2\}$. But the two subcells spanned by $\{e'_1, e'_2\}$ and $\{e_1, \varepsilon_2\}$ are flat and we can omit them, so that we obtain finally only two subcells whose union is a fundamental domain of \mathbb{Z}^2 . The corresponding tiling of the plane (gray area on Fig. 2) is the oblique tiling.

Observe that whatever the order of the decomposition, the resulting tiling is the same. Since each tile is the sum of the projection of a basis vector on \mathbf{E}_{\parallel} and of the projection of the other on \mathbf{E}_{\perp} , it is clear that any cut \mathbf{E}_c parallel to \mathbf{E}_{\parallel} which does not intersect the lattice inherits a tiling by means of the two projections e_1 and e_2 , which is our quasiperiodic tiling: in fact, the pieces of the boundaries of the tiles of the oblique tiling which are parallel to \mathbf{E}_{\perp} (which are called the existence domain of the corresponding tile) have by their very construction an union identical to the lattice $\tilde{\sigma}$ of atomic surfaces (which appear as the existence domains of vertices).

Due to its recursive character, the same argument works in any dimension n . Since we double the number of subcells each time we operate the decomposition $\varepsilon_i = e_i + e'_i$, we end with 2^n subcells. But only those which are spanned by d projections e_i of basis vectors on \mathbf{E}_{\parallel} and $(n - d)$ projections e'_i on \mathbf{E}_{\perp} have a non-zero volume and their number is $\binom{n}{d}$. As in the low dimensions case, one easily verifies that the traces of these subcells on \mathbf{E}_{\perp} , which are parallelotetra spanned by $(n - d)$ projections e'_i , exactly cover the atomic surface $\sigma_0 = \pi_{\perp}(\gamma_n)$ attached to the origin, so that our construction yields in the general case a tiling of the d -dimensional cut \mathbf{E}_c by means of the projections of the $\binom{n}{d}$ d -dimensional facets of the hypercube γ_n .

2.4.3. Octagonal tilings

The canonical octagonal (or Ammann) tiling, shown in Fig. 3, was first introduced by R. Ammann [17] and F. P. M. Beenker [18], and is obtained in a straightforward way as Penrose-like tilings with $n = 4$, $d = 2$, and the direction of the pair $(\mathbf{E}_{\parallel}, \mathbf{E}_{\perp})$ prescribed by the following symmetry considerations:

Consider a regular octagon in the Euclidean plane and choose four of its vertices, no two of them being opposite as shown on Fig. 4. Consider the four vectors joining the center of the octagon to these vertices. There exists a unique embedding of the plane in \mathbb{R}^4 such that the canonical orthonormal basis of \mathbb{R}^4 projects orthogonally on our four vectors. Now consider the symmetry group $8mm'$ of the octagon. Since it permutes the vertices of the octagon, we can define a 4-dimensional action of this group by the condition that it

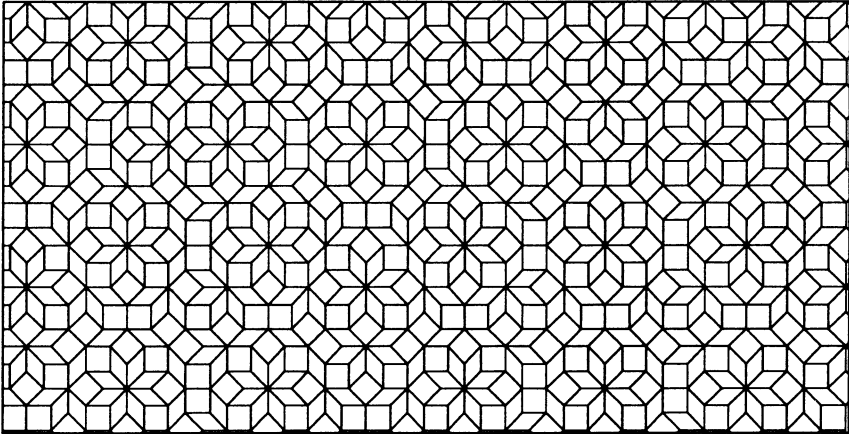


Fig. 3. — A sample of the Ammann octagonal tiling.

permutes the basis vectors in the same way as the vertices of the octagon, and since this action involves only signed permutations, the lattice \mathbf{Z}^4 spanned by the basis is preserved by this action. Then we decompose this representation of $8mm'$ into irreducible representations and find two of them, one carried by our embedded plane, which is identified with \mathbf{E}_{\parallel} , and the other by the orthogonal plane, identified with \mathbf{E}_{\perp} .

It is easy to see that the prototypic atomic surface $\pi_{\perp}(\gamma_4)$ is a regular octagon, and that the six 2-dimensional facets of γ_4 fall under π_{\parallel} on two orbits of tiles: two squares (with orientations differing by a $\pi/4$ rotation), and four rhombi with an acute angle of $\pi/4$, again mapped on each other by rotations which are multiples of $\pi/4$. Observe how the basis vectors $\{\varepsilon_1, \varepsilon_2, \varepsilon_3, \varepsilon_4\}$ project onto the parallel and perpendicular spaces. On the parallel space, they are de-

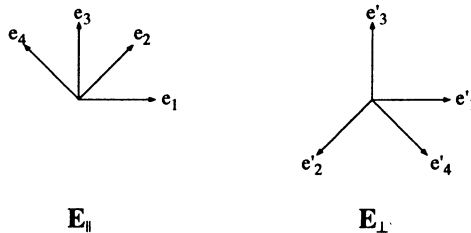


Fig. 4. — The orthogonal projection on \mathbf{E}_{\parallel} and on \mathbf{E}_{\perp} of the standard orthonormal basis ε_i , $i = 1, \dots, 4$ of \mathbb{R}^4 .

duced from each other by a rotation of $\pi/4$. In the perpendicular space, the projections of the same vectors are mapped on each other by a rotation of $5\pi/4$ (or $-3\pi/4$) as shown on Fig. 4.

3. THE COMPOSITION-DECOMPOSITION METHOD

3.1. Self-similarity

In some cases, there exist lattice-preserving linear transformations which commute with the two projections ($\pi_{\parallel}, \pi_{\perp}$). Such transformations are elements M of $Gl(n, \mathbf{Z})$ which preserve the subspaces \mathbf{E}_{\parallel} and \mathbf{E}_{\perp} .

Given a tiling associated to the canonical atomic surface $\pi_{\perp}(\gamma_n)$, one can construct a new atomic surface as $\pi_{\perp}M(\gamma_n)$, by taking the projection of the image through M of the unit hypercube. Since M preserves \mathbf{E}_{\parallel} and \mathbf{E}_{\perp} , it transforms any cut \mathbf{E}_c parallel to \mathbf{E}_{\parallel} into a parallel cut $M(\mathbf{E}_c)$ which carries the image under the restriction of M to \mathbf{E}_{\parallel} of the tiling carried by \mathbf{E}_c .

Of special interest is the case where M operates on \mathbf{E}_{\parallel} and \mathbf{E}_{\perp} by homotheties, since in this case the image of the tiling under M is a tiling of the same type, but at a different scale:

$$M = \lambda\pi_{\parallel} + \mu\pi_{\perp}; \quad \lambda, \mu \in \mathbf{R} \quad |\lambda\mu| = 1$$

This happens in particular when there is an invariance point group of the high-dimensional lattice, such that \mathbf{E}_{\parallel} and \mathbf{E}_{\perp} are the only two invariant subspaces, carrying irreducible non-equivalent representations of the invariance group.

Let us give an explicit example with the octagonal tiling. A simple examination of the projection of the canonical basis onto \mathbf{E}_{\parallel} and \mathbf{E}_{\perp} shows that $e_1 + e_2 + e_3 = (\sqrt{2} + 1)e_2$ in \mathbf{E}_{\parallel} while $e'_1 + e'_2 + e'_3 = -(\sqrt{2} - 1)e'_2$ in \mathbf{E}_{\perp} . This suggests to construct the matrix:

$$M = (\sqrt{2} + 1)\pi_{\parallel} - (\sqrt{2} - 1)\pi_{\perp} = \begin{pmatrix} 1 & 1 & 0 & -1 \\ 1 & 1 & 1 & 0 \\ 0 & 1 & 1 & 1 \\ -1 & 0 & 1 & 1 \end{pmatrix}$$

M is easily seen to have all the required properties: it belongs to $Gl(4, \mathbf{Z})$, its determinant is 1 and it commutes, by construction, with the action of the octagonal group, so that it reduces on \mathbf{E}_{\parallel} to a dilatation of ratio $(\sqrt{2} + 1)$ and on \mathbf{E}_{\perp} to a contraction of ratio $(1 - \sqrt{2})$. Notice that such a matrix M exists also in the icosahedral case. The corresponding "inflation" and "deflation" ratios are $2 \pm \sqrt{5}$.

Now, our general argument shows that if we replace our original atomic surface by an octagon $(\sqrt{2} - 1)$ times smaller, then we will find in any cut an octagonal tiling scaled by a factor $(\sqrt{2} + 1)$. In particular, if we consider both atomic surfaces: our original one containing the smaller one, we see that we

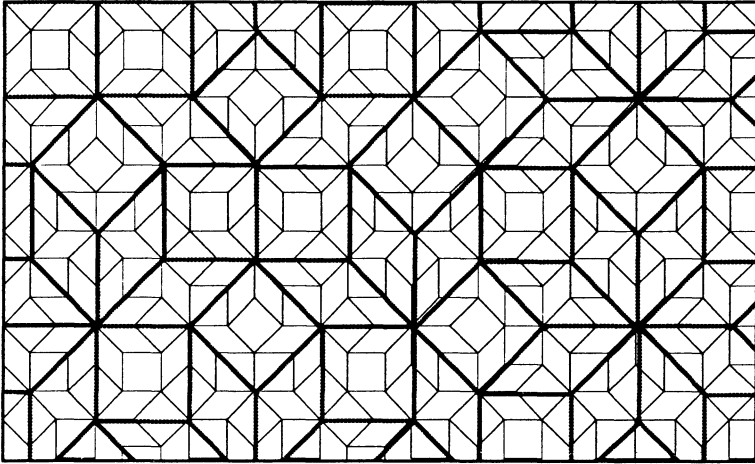


Fig. 5. — A sample of the octagonal tiling, showing some deflated tiles.

can “extract” from any tiling the vertices of a larger one, by discarding all the vertices which correspond to intersections of the cut with the large octagon, falling outside the small one, as shown on Fig. 5. In the cut, one can describe this operation as the regrouping of clusters of tiles to form larger tiles, and this is called a *deflation*. Since the matrix M is invertible, this process may be done in the reverse way: it is possible to “dissect” the tiles of a given tiling, in order to obtain a tiling of the same type, but with an edge length shortened by a factor $(\sqrt{2} - 1)$. This is called an *inflation*, because it enlarges the number of the tiles.

Observe that for these considerations we are not interested in comparing the tiling carried by E_c and $M(E_c)$, because the “absolute” position of the cut is in general difficult to assess (due to the so-called local isomorphism property, see for instance [19]) unless the tiling has special (global) symmetry properties. On the contrary, we are interested in comparing two tilings carried by the same cut. This entails that the position of the small atomic surface inside the large one is irrelevant: whatever this position, the discarding process explained above will lead to a “deflated” tiling. We conclude that generally the inflation/deflation constructions are not uniquely defined, although they usually become unique if some further natural requirements are imposed.

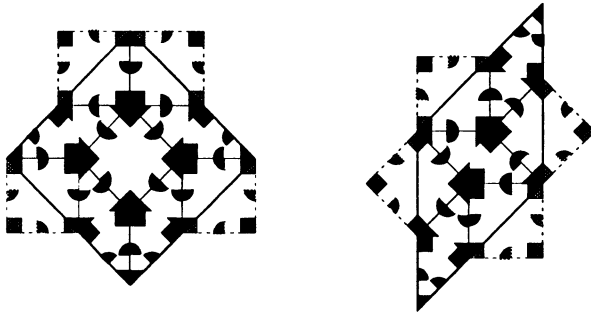


Fig. 6. — Composition and decomposition for the Ammann decoration of the octagonal tiling

3.2. Inflation and quasiperiodicity

In order to describe these additional requirements, let us first consider the inflation process. A natural requirement is that the (globally defined) inflation can be described by a “local” dissection of tiles into smaller ones, which means that the dissection follows rules (the decomposition rules) which are purely local in the sense that the dissection of each tile depends only on a *finite* neighbourhood of the tile. If we require furthermore that the decomposition rules are compatible with symmetry, by treating symmetry-related tiles in a symmetry-related way, inflation usually becomes unique. In the case of the octagonal tiling, this latter requirement implies that the octagonal atomic surface for the initial tiling and its inflation are concentric.

For what follows, it is important that the global and the local definitions of inflation define the very same inflation process. The local definition of inflation can therefore be used as a tool to generate the tiling: one simply starts with a finite seed, for instance reduced to one tile, and repeatedly applies the inflation or decomposition procedure, followed each time by a rescaling so as to maintain the same size for the tiles. In this way, a tiling of any desired size may be constructed. This method has been used in particular when no global methods were available (R. Penrose [5], L. Danzer [20]) or when the atomic surfaces are fractal (P. Stampfli [21], E. Zoretz [22]).

So far, we have considered a local definition only for inflation. In many cases, however, deflation also allows for a local definition, through local rules following which one can build “supertiles” from clusters of original tiles (composition rules). As for the decomposition rules, locality means here that the composition rules should depend only on a *finite* neighbourhood of the cluster. However, locality of deflation is a much less trivial property than locality of inflation.

Now, if both inflation and deflation allow for a local definition, they can be used to prove that a properly chosen set of matching rules enforces the quasiperiodicity of any tiling in which these rules are satisfied everywhere.

Let us illustrate this on the case of the octagonal tiling carrying the Ammann decoration depicted on Fig. 12 in section 5 where the origin of this decoration is explained. Given the Ammann decoration, the composition and decomposition rules can be described in a very local way, as shown on Fig. 6. In fact, one can show (see [27]) that any tiling admitting the Ammann decoration (i. e., satisfying the matching rules) has a unique composition and a unique decomposition (whether it is quasiperiodic or not). This is the key property for proving that the matching rules enforce the quasiperiodicity of the tiling.

Let \mathcal{T} be any tiling carrying the Ammann decoration, and let us consider a finite, but otherwise arbitrary patch \mathcal{P} from \mathcal{T} . We can apply repeatedly the (unique) composition process to \mathcal{P} , until it is so small that it is obviously a piece of a quasiperiodic tiling (notice that all the vertex neighbourhoods allowed by the matching rules do occur in the quasiperiodic tilings, as can be checked by inspection). But since composition and decomposition are unique and inverse of each other, we can conclude that \mathcal{P} itself must be a piece of a quasiperiodic tiling. Since this is true for any finite \mathcal{P} , we have shown that \mathcal{T} must be quasiperiodic.

The procedure described above is actually a method (see [3]) to prove that a certain set of matching rules enforces quasiperiodicity. It has been explicitly or implicitly used by many authors, including N. G. de Bruijn [6], J. E. S. Socolar [23], F. Gähler [3], R. Klitzing, M. Schlottmann and M. Baake [24] [25] and probably others. The key requirement for this method to work is that both inflation and deflation are unique and local, and that they are defined for all tilings satisfying the matching rules.

4. THE METHOD OF FORBIDDEN PLANES

We switch now to a quite different approach to the theory of matching rules.

4.1. Position of the problem

Let us first observe that, given a canonical tiling and its prototiles as suitable projections of facets of the hypercube, it is quite possible to describe *any* tiling made of the same prototiles with a cut through the same lattice of atomic surfaces used for obtaining the quasiperiodic tiling: in fact, we can distinguish between the subspace \mathbf{E}_{\parallel} on which is built the tiling and the cut \mathbf{E}_c used to select the vertices of the high-dimensional lattice which are projected on the vertices of the tiles. As soon as the direction of \mathbf{E}_{\perp} , considered as the carrier of the atomic surfaces and the direction of the projection on \mathbf{E}_{\parallel} , is irrational with respect to the lattice, it is clearly possible to lift in a unique way each vertex of an arbitrary tiling on a vertex of the lattice. Then it is possible to dissect the tiles in simplices (triangles in two dimensions, tetrahedra in three and so one) and to lift these simplices to linear affine simplices of \mathbb{R}^n in order to get a “faceted” cut which selects the relevant vertices (if it happens that this cut

intersects additional atomic surfaces, it is quite clear that it is always possible to distort locally the cut in order to remove the extra intersections). Of course, the cut is not uniquely defined: *any* cut which goes through the same set of atomic surfaces selects the same set of vertices and defines the same tiling, as exemplified on Fig. 7.

Since our atomic surfaces are topologically balls, it is easy to show that two cuts define the same tiling if it is possible to distort continuously one cut until it becomes equal to the other without crossing the boundary of any atomic surface: in mathematical terms, we say that a tiling is defined by a **homotopy class of cuts** in the complementary of the boundaries of the atomic surfaces. The special property of our quasiperiodic tilings is that this homotopy class *contains a plane* (up to now, we have considered mainly these planes), so that the problem of proving that a given matching rule enforces the quasiperiodicity is to show that every homotopy class of cuts compatible with this rule contains a plane. As we shall see, the direction of this plane cannot be arbitrary.

Our strategy to deal with this problem is best explained by referring to the low dimensional model of Fig. 1. We accept now as a cut any line projecting one-to-one on E_{\parallel} along E_{\perp} and we may distort it as we want as long as the cut does not cross any endpoint of an atomic surface. How could we impose through local constraints that such a homotopy class of cuts contains a straight line? A first step in this direction is provided by the oblique tiling (see Fig. 2). As is easily seen, the requirement of getting whole tiles upon projection (i. e., to get only the two projections of the edges of the canonical square in the projected structure on E_{\parallel}) is achieved if we impose that the cut *does not intersect* the components of the boundaries of the oblique tiles which are parallel to E_{\parallel} . Of course, this constraint does not forbid the cut from wandering very far, but nevertheless results in a kind of *local channelling* of the cut, of which we are looking for a global counterpart.

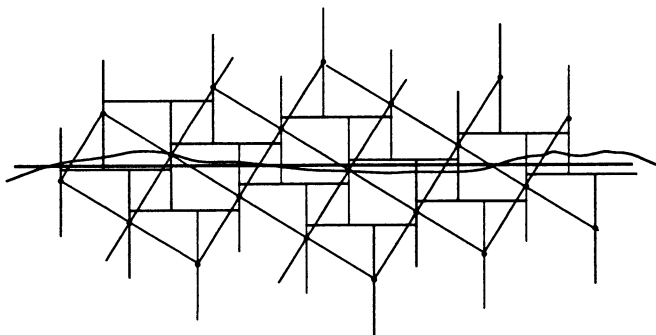


Fig. 7. — The curved cut drawn here can be continuously distorted to a straight line while generating the same tiling: all curves generating the same tiling belong to the same homotopy class (see text).

The most natural idea is then to enlarge the line segments that the cut is forbidden to cross and to see what happens: in fact, there are only two possible situations. The first one corresponds to rational values for the slope of \mathbf{E}_{\parallel} . In such a case, for a certain *finite* enlarging, the endpoints of our line segments will connect and the resulting lines divide the plane into parallel stripes. A homotopy class of cuts is made of all possible cuts confined in one of these stripes and contains evidently straight lines. The corresponding tilings are obviously periodic.

The other case corresponds to irrational values for the slope of \mathbf{E}_{\parallel} . Then, whatever large is the finite enlargement we make on the segments, they will never connect and nothing happens: we do not obtain a global channelling in this way.

These considerations may look somehow disappointing, since all we get is that we may define matching rules in this way only for periodic tilings. However, they are the real key to the theory of matching rules in higher dimension, where the “special” directions which allow this machinery to results in matching rules are not only the rational ones. We shall now discuss that point.

4.2. Non-transversality conditions

In higher dimension too, we can make such a rough classification: if \mathbf{E}_{\parallel} is a d -dimensional subspace in \mathbb{R}^n , we classify the directions of \mathbf{E}_{\parallel} by the rank of the sublattice of $\mathbb{Z}^n \in \mathbb{R}^n$ which falls on \mathbf{E}_{\parallel} . This rank is d for a “completely rational” subspace associated with periodic tilings, and more generally it is the number of dimensions along which the tiling is periodic. In the “completely irrational” case in which we are interested, cuts parallel to \mathbf{E}_{\parallel} go through at most one vertex of \mathbb{Z}^n . Observe that this is equivalent to the fact that the projection of \mathbb{Z}^n on \mathbf{E}_{\perp} along \mathbf{E}_{\parallel} is uniformly dense (and notice that this is independent on the direction of \mathbf{E}_{\perp} , which is involved here only as the quotient $\mathbb{R}^n/\mathbf{E}_{\parallel}$).

However, this rough classification does not describe sufficiently the situation and we have to introduce a finer one. The idea is to consider the projection on \mathbf{E}_{\perp} of the lattice subspaces of dimension t greater than or equal to $(n - d)$ (the dimension of \mathbf{E}_{\perp}). For an arbitrary direction of \mathbf{E}_{\parallel} , the projection covers \mathbf{E}_{\perp} . But for special directions of \mathbf{E}_{\parallel} , there may exist one or several lattice subspaces whose projections “lose dimensions” and does not cover \mathbf{E}_{\perp} . Of course, this is the case for the completely rational case, but the important point is that such situations may also occur in the completely irrational case. In fact, the corresponding property of \mathbf{E}_{\parallel} is that it is *not transversal* to a lattice plane and this does not require \mathbf{E}_{\parallel} to be itself, partially or completely, rational.

This fact is indeed widely used in quasicrystallography of icosahedral phases: all 2-dimensional rational planes spanned by any two integer vectors ξ and $M(\xi)$ of \mathbb{Z}^6 , where M is the inflation matrix (section 3.1), are not transversal to \mathbf{E}_{\parallel} : their projection on \mathbf{E}_{\parallel} are equal to their traces on \mathbf{E}_{\parallel} . For example, 5-, 2- or 3-fold symmetry 2-dimensional planes project on \mathbf{E}_{\parallel} along lines and

not on planes as would be expected in a generic case. This exceptional non-transversality is the basis of the definition of “rows” and “reticular planes” in the quasicrystallography of the icosahedral phases (see for instance [26]).

In such a non-transversal situation, the projection of \mathbf{Z}^n on \mathbf{E}_\perp acquires some extra structure: not only this projection is dense in \mathbf{E}_\perp , but its trace on the projection of the non transversal lattice subspace is also somewhere dense since this projection, which contains a module of rank t , has a dimension lower than t .

This is the situation in which non trivial matching rules may exist. Rather than developing the general theory in an abstract way, we shall explain with sufficient details the case of the octagonal tiling, which is the most simple case but contains all the main ideas, and moreover is very close to the icosahedral case of physical interest.

4.3. The forbidden planes

Like in the low dimensional model, let us consider the oblique tiling associated with the octagonal tiling and explore it by shifting the cut. When the cut is in a generic position, then it intersects the boundaries of the oblique tiles only on parts parallel to \mathbf{E}_\perp and we see in the cut a regular tiling. But when we let the cut hit the boundary of one atomic surface, then it intersects around that point parts of the boundaries of the oblique tiles which are parallel to \mathbf{E}_\parallel : namely we see in such a special cut “a flipping hexagon, at the instant where it flips”. As already observed, to forbid a cut to cross such parts of the boundary of the oblique tiles forces it to select whole tiles.

Now, the remarkable point is that in such a special cut, we find not only one flipping hexagon, but a whole infinite family aligned along a so-called “worm” (Fig. 8). This comes from the fact that there are translations in \mathbf{Z}^4 which project on \mathbf{E}_\perp along the boundary of the atomic surface, and these projections fill densely the carrier of this boundary.

To be more specific, let us consider the segment of the boundary of the octagon parallel to e'_1 . Its carrier is the projection of a plane P parallel to the lattice plane spanned by $(\varepsilon_1, \varepsilon_2 - \varepsilon_4)$. But this carrier is also the intersection of P with \mathbf{E}_\perp , so that we find in P a rectangular lattice of segments parallel to e'_1 .

On the other hand, our special cut intersects P along a line parallel to e_1 . Thus we get exactly the situation of our low dimensional toy-model: a lattice (here rectangular) of atomic surfaces (the segments e'_1 bounding the octagon) irrationally oriented with respect to the lattice, and a cut (here a line parallel to e_1) also irrationally oriented: we conclude that we have a quasiperiodic distribution of intersections between the cut and the segments, which, viewed in the four dimensional space, is a set of intersections of the special cut with boundaries of octagons. They are aligned along a straight line and separated by finite distances. Each of them belongs to pieces of boundaries of oblique tiles, whose traces in the cut build the “flipping hexagons”. These hexagons

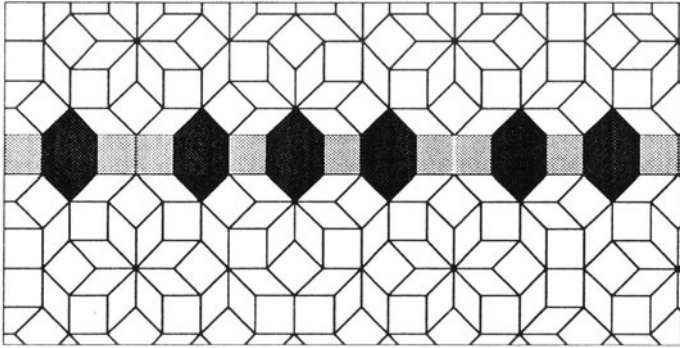


Fig. 8. — Infinite family of flipping hexagons defining a “worm” of the first kind in the octagonal tiling

are separated by one or two squares.

Observe that this highly non generic situation is the consequence of *two distinct features* of the construction of the octagonal tiling.

On one hand, the two planes \mathbf{E}_\perp and \mathbf{E}_\parallel , whose direction is forced by the octagonal symmetry, are non transversal to a set of lattice planes, specially those of the kind $(\varepsilon_1, \varepsilon_2 - \varepsilon_4)$, but they are infinitely many of them (and in fact we shall need another family to make the matching rules). These planes project on lines on \mathbf{E}_\perp and the two-dimensional lattice which they contain densely fills the projection. This non-transversality property accounts for the fact that in the plane P , the cut yields a one-dimensional trace and that the given intersection between the cut and the boundary of an atomic surface yields a whole lattice of such intersections.

On the other hand, it is because the boundary of the atomic surface is made of segments *contained* in planes like P that we find in P a lattice of segments. Would this segment be replaced by a curve in \mathbf{E}_\perp , the plane P would still touch a lattice of atomic surfaces as soon as it touches one, but it would touch them on points instead of whole segments, so that the trace of the cut in P would not intersect more than one of them.

Now we shall apply the naive idea stated in the introduction to this section: we shall “fill the holes” between the flipping hexagon by means of decorations which result in the dissection of the tiles of the oblique tiling and thus in an enlargement of the number of their boundaries. Deferring the explicit construction to the next section, let us first examine what will be the topological result of this construction.

In fact, the geometry of the boundaries “parallel to \mathbf{E}_\parallel ” of the oblique tiling is not very simple. They are three dimensional facets extending for two dimen-

sions in \mathbf{E}_{\parallel} and for the other one in \mathbf{E}_{\perp} . To see how they glue together, let us move our special cut: for a given position, we see in the cut a continuous worm made of flipping hexagons and of squares coming from the decoration. When we move our cut, we recover a regular cut unless we move along e'_1 , in which case we keep the worm, whose precise structure changes with the shift of the cut along e'_1 , according to the change of the structure defined by the restricted cut construction in the plane P .

For each position of the cut, the worm covers completely its symmetry axis, which is a line parallel to e_1 so that when we shift the cut along e'_1 , we see that the sets of facets covers completely a plane spanned by e'_1 and e_1 , which is parallel to our plane P . Thus we see that this set of facets is a complicated “thickening” of a very simple object: a two-dimensional lattice plane, suitably shifted. Finally, observe that it is equivalent to ask for the non-intersection of the cut with the set of facets, or with the plane on which this set can be “retracted” (i. e., flattened).

Thus the final form of our constraint will be the non intersection of the cut with a family of lattice planes, which we call forbidden planes. Before explaining the consequences of such a constraint, let us describe how a suitable decoration of the tiles together with a matching rule may be equivalent to the constraint for the cut not to cross the forbidden planes.

5. DECORATION OF THE TILES

In this section, will shall describe the decoration scheme first devised by R. Ammann for his octagonal tilings. This is not the only possible decoration (decorations are never unique) and perhaps not the simplest. However, this choice presents the advantage of involving many different topics of this kind of construction.

5.1. A simple case

Although there is no mathematical difficulty in the constructions that we are making, their description may be obscured by the fact that they rely entirely on the geometry of the oblique tiling, which is intrinsically four dimensional and not so easy to visualise.

Our first step is to explain why there are holes in the worm which appears in the special cuts going through the boundary of one octagon (and thus of a whole infinite quasiperiodic set of them). Recall that the boundaries of the oblique tiling we are interested in are made of the sum of a tile and of a segment of the boundary of its existence domain. Consider for instance the square belonging to the flipping hexagon spanned by (e_2, e_3, e_4) , which is the “vertical” hexagon. This square is (e_2, e_4) so that its existence domain is the square (e'_1, e'_3) . If the cut touches an atomic surface along e'_1 , say on the point x , the relevant piece of the boundary of the oblique tiling is the cube (e_2, e_4, e'_1) .

Now, consider one of the squares (e_1, e_3) touching this flipping hexagon along the worm (Fig. 9). It has a vertex v shifted from the flipping point x by e_2 , so that the cut pierces the atomic surface of v in the existence domain (e'_2, e'_4) of our square on a point on a diagonal of this existence domain. Since this diagonal does not belong to any boundary of the oblique tiling, our square is a regular one and does not belong to the forbidden set: in that sense, it is a hole in the worm.

Thus we see that in order to fill this kind of holes and make the whole worm a forbidden set, we have to dissect the oblique tiles corresponding to squares into several sub-tiles in such a way as to introduce as a new type of boundary the sum of a square of the tiling with the *diagonals* of its existence domain. This is readily achieved through the simplest decoration of the edges of the tilings, which consists in attaching an orientation to them.

Consider the existence domain of the origin of an edge, say e_3 , which is a "horizontal" hexagon inscribed in the bottom of the octagonal atomic surface. Let us cut this hexagon into two parts along its long (horizontal) diagonal (Fig. 10) and let us decide to associate an arrow pointing upward to each edge whose origin falls in the bottom half of the hexagon, and pointing downward for those whose origin falls in the other half. Now observe that this decoration is compatible with the symmetries of this edge: namely, the vertical symmetry axis preserves each decorated subdomain, while the associated operation in \mathbf{E}_{\parallel} exchanges the two sides of the edge (so that the arrow have to be symmetric with respect to the direction of the edge). Concerning the horizontal symmetry axis, the situation is slightly more subtle. This axis maps the existence domain of the origin of the edge to the existence domain of its extremity, while the associated operation in \mathbf{E}_{\parallel} exchanges the two end-points of the edge. To get a symmetry compatible decoration, we thus have to put a downward arrow in the upper half of the upper hexagon and an upward one in the other half. Then we verify that we have actually defined an orientation for the edge, since a given edge is oriented in the same way, viewed from its origin or viewed from its extremity. Then we can set the decoration of the other edges, using associated symmetry operations in \mathbf{E}_{\perp} and in \mathbf{E}_{\parallel} .

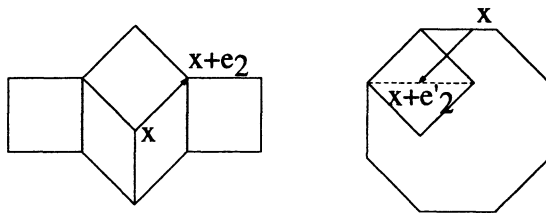


Fig. 9. — The vertices of the squares close to a flipping hexagon fall on the diagonal of their existence domains.

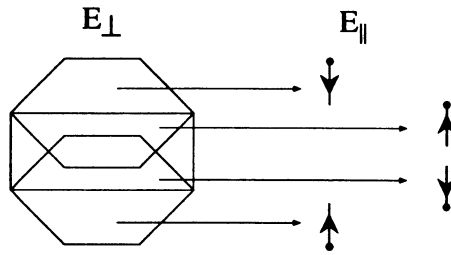


Fig. 10. — The orientation of the edges corresponds to the dissection of their corresponding existence domains.

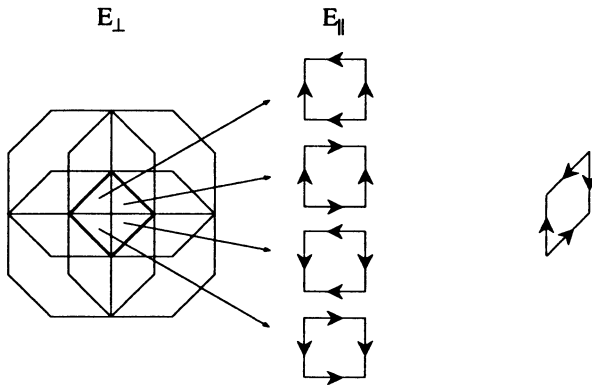


Fig. 11. — The decoration of the square induced by the decoration of the edges (left); the unique decoration of the rhombus (right).

Now we come to the corresponding decoration of the tiles themselves, which amounts to superimpose the atomic surfaces corresponding to the vertices of the tiles, shifting them as required, and to study how the existence domains of tiles are partitioned in existence domains of decorated tiles (Fig. 11). What we find is that the existence domain of the rhombi are not partitioned, so that we get immediately only one kind of arrowed rhombi, with the arrows pointing to the obtuse angles. On the contrary, the domain of the squares are partitioned in four decorated subdomains by their two diagonals, and that is what we were looking for. Observe however that, although there are four subdomains, there is only one decorated square, characterised by the fact that parallel edges are given the same orientation. But this unique square is attached in different orientations to each of the subdomains.

It remains to see what is the matching rule and how it works. The matching rule itself is trivial in this context: it requires to fit tiles together with the same orientation for the shared edges (what is trivial is that within the cut

construction, each edge is in fact selected only once, together with its arrow (if it is arrowed). But we have to show why it is forbidden to cross the new “internal” boundaries of the decorated oblique tiling (recall that it is forbidden to cross the original boundaries in order to get only whole tiles in the cut). Now, the point is simply that if we allow a cut to enter into an oblique tile through an edge of a given orientation, and then to cross the internal boundary corresponding to this orientation, then it will leave the oblique tile through an edge having the opposite orientation, and we would get a *wrongly decorated tile*. If we insist to make a tiling with only our “well decorated” tiles, then we forbid the cut to cross these new boundaries. Notice in particular that in this context, a “fault” is not the mismatch of decorations, which means nothing as long as we use continuous cuts. It is the occurrence of an improperly decorated tile.

To sum up, we have set simple decorations of the edges, obtaining one decorated rhombus and one decorated square, such that making a tiling with these two tiles alone and matching decorations corresponds to use a cut which does not intersect the family of forbidden planes made of four lattices of 2-dimensional lattice planes spanned respectively by $(\varepsilon_1, \varepsilon_2 - \varepsilon_4)$, $(\varepsilon_2, \varepsilon_1 + \varepsilon_3)$, $(\varepsilon_3, \varepsilon_2 + \varepsilon_4)$ and $(\varepsilon_4, \varepsilon_3 - \varepsilon_1)$.

Alas, this is not sufficient to get the octagonal quasiperiodic tilings (although the edge decoration yields matching rules! see section 7). The reason for that is quite clear. Recall that the directions of \mathbf{E}_{\parallel} for which we may have matching rules are required to be non transversal to a set of lattice planes. But there are infinitely many directions of planes which are non transversal to the four above-mentioned directions. More precisely, there is a one parameter family of them, which all possess the symmetry of the square, and only two of them have in addition the full octagonal symmetry. Thus, in order to get matching rules for the octagonal tiling, we need to add more forbidden planes in order to get a set such that our \mathbf{E}_{\perp} and \mathbf{E}_{\parallel} will be the only planes non transversal to this set.

5.2. The Ammann decoration of vertices

The strategy is clear: pick suitable other lattice planes, and devise decorations such that using only these new decorated tiles corresponds to not crossing these planes, i. e., defines them as forbidden planes.

In order to illustrate various aspects of this theory, and to honour the cleverness of R. Ammann (see [17]), we shall sketch the description of his decorations (and finally show that they enforce the quasiperiodicity, a result which may also be obtained from a self-similarity approach, as we have already seen).

First, the choice of the new planes. Besides the planes which project on \mathbf{E}_{\parallel} and \mathbf{E}_{\perp} on the same directions as the basis vectors, it is natural to try those which fall on the bisectors of them, because these bisectors are simple directions (diagonals of the rhombi) and correspond also to the diagonal of the octagon. Thus we choose the planes spanned respectively by $(\varepsilon_1 + \varepsilon_2, \varepsilon_3 - \varepsilon_4)$,

$(\varepsilon_2 + \varepsilon_3, \varepsilon_1 + \varepsilon_4)$, $(\varepsilon_3 + \varepsilon_4, \varepsilon_2 - \varepsilon_1)$, $(\varepsilon_4 - \varepsilon_1, \varepsilon_3 - \varepsilon_2)$. It is a matter of simple algebra to verify that the only planes simultaneously non transversal to the whole set of eight directions of planes are our \mathbf{E}_\perp and \mathbf{E}_\parallel .

Second, the decoration. It is a vertex decoration, defined through a partition of the atomic surface (existence domain of a vertex) much like the previous edge decoration was defined through a partition of the existence domains of edges. Thus, we divide the octagon in eight sectors by the diagonals running from a vertex to the opposite one, and we attach to each sector a mark, arbitrary excepted for the fact that it should have the same symmetry as the sector (a symmetry axis parallel to a basis vector). Let us choose for the moment the generic shape depicted on the upper left of Fig. 12. We complete the decoration of the other sectors using symmetry.

Third, we examine how many different decorated tiles we get. As usual (see [19]), we superimpose suitably shifted copies of the octagon and we study the decomposition of the existence domain of each tile in subdomains of decorated tiles. What we find is that there are many of them, so that we get a lot of decorated tiles and this does not look very pretty. However, this complication is inessential and we can simplify the decoration using a “reduction trick” that we shall now explain.

Let us proceed by steps. Initially, we have a generic mark attached to each vertex and the matching rule consists in putting tiles around each vertex in such a way that the marks coming from the different tiles coincide. Observe that since the mark is attached to the vertex, it overhangs the edges of the tiles. We can give an alternative form to the matching rule by attaching to each vertex of tile only the trace of the mark on this tile, and ask to recompose the shape of the mark around each vertex. Clearly, these two forms of the matching rule are equivalent as long as the trace of the mark on the tile gives sufficient information to reestablish the whole mark, and that is the case if the shape of the mark is generic enough.

Next, we can modify and specialise the shape of the mark in such a way that *some* traces of our mark become identical. To see the effect of this procedure, consider two adjacent subdomains of existence in the existence domain of a tile. The internal boundary between the subdomains is there because at some vertex the tile bears the mark in two different orientations for the two subdomains. If we modify the mark up to identify its trace on the tile for these two different directions, then we can no longer make any distinction between the two subdomains and this amounts to *rub out* the corresponding internal boundary.

This is a way to simplify the decoration and to decrease the number of decorated tiles. Of course, one has to be careful not to go too far: to put a disk on each vertex is obviously equivalent to no decoration at all A remarkable property of the octagonal tiling is that there is a class of shapes for the mark, among which the Ammann’s “large arrow”, which yield an effective decoration with only one decorated square and two decorated rhombi (which are mirror images of each other, see Fig. 12). We get only one decorated

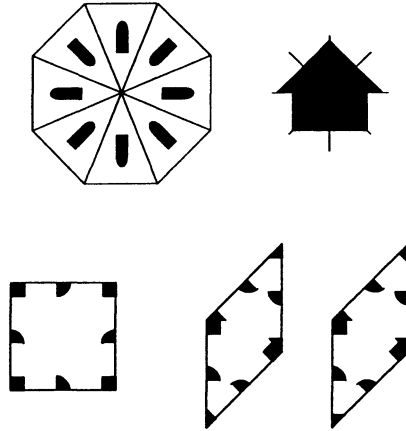


Fig. 12. — A generic vertex decoration for the octagonal tiling (upper left). The Ammann arrow is a special distortion of this generic mark (upper right) which leads to three kinds of decorated tiles. Complete Ammann and edge decorations of the octagonal tiling (bottom).

square, because we have rubbed out all the internal boundaries. Those which survive in the existence domain of the rhombus are easily seen to be the two diagonals: two opposite triangles correspond to the same decorated tile, and the two diagonals are symmetry axes associated in \mathbf{E}_{\parallel} to two symmetry axes. Each of them exchanges the two decorated rhombi.

Now, we have to see that these internal boundaries of the existence domains of the rhombi are sufficient to provide us with the required supplementary set of forbidden planes. To fix the notations, let us consider a special cut piercing an atomic surface somewhere on the diagonal spanned by $e'_1 - e'_2$ (or $e'_3 + e'_4$). Then this cut will pierce also a whole quasiperiodic set of atomic surfaces along the same diagonal. Since this cut hits the internal boundary (the long diagonal) of the rhombus (e'_1, e'_2) , which is the existence domain of the rhombus (e_3, e_4) , we see in the cut these rhombi as traces of the boundaries of the decorated oblique tiling, and similarly for the rhombi (e_1, e_2) through the short diagonal of its existence domain (e'_3, e'_4) . To see that this set of rhombi covers completely its axis (a line parallel to $e_1 - e_2$), let us build the restriction of our four dimensional cut construction to the lattice plane $(\varepsilon_3 + \varepsilon_4, \varepsilon_2 - \varepsilon_1)$ which intersects our special cut along a line. We just have to observe that the trace of the atomic surface in this plane, which is its diagonal, is exactly the projection on the trace of \mathbf{E}_{\perp} of the unit rectangle of the two dimensional lattice to conclude that we are again exactly in the situation of the low dimensional model and that this restricted cut construction yields a tiling of the trace of the special cut by means of the two projections of the basis vectors, which are nothing but the diagonals of our rhombi.

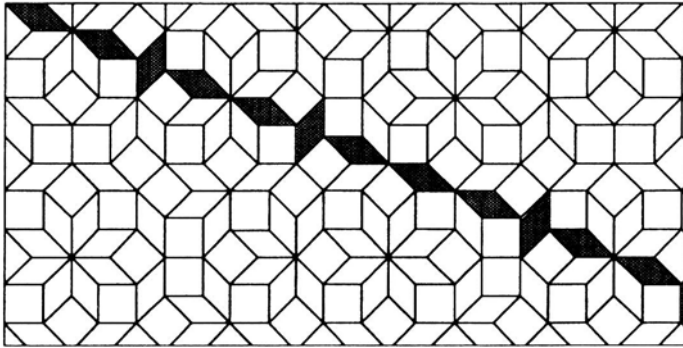


Fig. 13. — A worm of the second kind in the octagonal tiling.

Thus we get a “worm of the second kind” made uniquely of rhombi, which does not have holes and covers completely its axis (Fig. 13). Moving the special cut along the direction $e'_1 - e'_2$ of the diagonal shows as previously that the whole plane $(\varepsilon_3 + \varepsilon_4, \varepsilon_2 - \varepsilon_1)$ is contained as a retract in the boundaries of the decorated oblique tiling. On the other hand, the fact that this plane is forbidden results of the same considerations already made: would the cut cross the internal boundary, this would result in an improperly decorated rhombus.

Finally, the whole set of decorations for the octagonal tiling is the superimposition of the orientation of the edges (Ammann used half-disc rather than arrows) and of the vertex decoration. The matching rules require that two adjacent tiles give the same orientation to their common edge and that the mark on the vertices fit together to form the large arrow. We know that this set of constraint is equivalent to the non-intersection of the cut and the forbidden planes. We shall now prove that this entails the quasiperiodicity of our tilings.

6. THE MAIN THEOREM

For this, we first need more information about the position of the forbidden planes with respect to the lattice, and about their intersections.

6.1. Position and intersections of the forbidden planes

Setting once for all the positions of the atomic surfaces such that their centers are on the vertices of the lattice \mathbf{Z}^4 , let us begin by the second set of planes corresponding to the vertex decoration: since they intersect octagons along a diagonal, they go through the vertices of \mathbf{Z}^4 . It is a matter of simple algebra to

study their intersections. One finds that they intersect all four on the vertices of the lattice and on the body centers, and that in addition each pair of planes which are orthogonal in both projections in \mathbf{E}_\perp and \mathbf{E}_\parallel intersects on a face center.

Concerning the first family, consider a “horizontal” worm parallel to e_1 . The corresponding forbidden plane is parallel to $(\varepsilon_1, \varepsilon_2 - \varepsilon_4)$ but does not go through the lattice from which it is shifted twice: first, this plane passes on the boundary of the atomic surface and thus is shifted from its center by $(-e'_2 + e'_3 - e'_4)/2$. Second, it is shifted to the axis of the worm. To compute this shift, observe that after the first shift the plane goes through the flipping points of the hexagons of the worm, so that we have to shift it to the middle between the flipping point and its image under the flip, which are symmetrical with respect to the axis of the worm. Since the jump vector is $e_3 - (e_2 + e_4)$, the last shift is $(-e_2 + e_3 - e_4)/2$ so that the total shift from the vertex is $(-\varepsilon_2 + \varepsilon_3 - \varepsilon_4)/2$. Now the plane itself contains $\varepsilon_1/2$ and we conclude that these planes go through the body centers of the lattice. Then one computes easily that they intersect all four on the body centers and that like in the previous case the “orthogonal” pairs intersect also on face centers. Finally, any two planes coming from the two families intersect only on a body center.

The conclusion is thus that we have three kinds of intersections: pairs of “orthogonal” planes coming from both families on the face centers, quadruplets of the second family on the vertices, and octuplets of all planes on the body centers.

Our problem is now mathematically clean: we have to show that any cut (everywhere transversal to \mathbf{E}_\perp) which does not intersect any forbidden plane is homotopic to a plane parallel to \mathbf{E}_\parallel . To begin with, we give the following description of the homotopy classes in question.

6.2. Systems of data

Let us describe the cut by its intersection with each of the fibers of the projection π_\parallel on \mathbf{E}_\parallel (the fiber above the point $x \in \mathbf{E}_\parallel$ is the plane parallel to \mathbf{E}_\perp which intersects \mathbf{E}_\parallel on x). It is very important to observe that, due to the non-transversality of the forbidden planes with respect to \mathbf{E}_\perp , the trace of the forbidden planes on each fiber $\pi_\parallel^{-1}(x)$ is not a point for any x as is the generic case for two (two-dimensional) planes in \mathbb{R}^4 . On the contrary, we have for each forbidden plane the following situation: the plane projects on \mathbf{E}_\parallel along a line, and if x does not belong to this line, then there is no intersection between the plane and the fiber. When x belongs to this line, then the forbidden plane intersects the fiber along a line. Finally, it is easy to observe that when x is the intersection of the projections of several forbidden planes, then the corresponding lines in the fiber also intersect on a common point.

This situation allows a very simple description of the homotopy class of the cut, which is transversal to \mathbf{E}_\perp and thus intersects each fiber on exactly one point: we have only to specify, for every $x \in \mathbf{E}_\parallel$, through which connected

component of the complementary of the trace of the forbidden planes goes the cut. This is what we call a *system of data*. The data are of three possible types: first, for almost all x , the fiber does not intersect any forbidden plane and there is only one connected component to choose (the whole fiber). Second, for a x which lies on the projection of a single forbidden plane, the fiber is divided in two half-planes by its intersection with the forbidden plane and we have to choose one of them. Finally, if several forbidden planes are involved, they define in the fiber a set of sectors around their common intersection and we have to choose one of them.

It is now almost obvious that systems of data defined by continuous cuts are in one-to-one correspondence with the homotopy classes of cuts. In fact, consider two cuts defining the same system of data. This means that in every fiber their traces belong to the same connected component of the complementary of the traces of the forbidden planes. Since these components are convex, we can draw in each fiber the line segment between the traces of the two cuts, being sure that this segment does not intersect the forbidden planes. Then, we can interpolate between the two cuts along these segments in order to define a homotopy from one cut to the other. Reciprocally, if for at least one fiber the two cuts fall in different connected components, then it is quite clear that it is not possible to distort continuously one to the other without crossing one or several forbidden planes.

Thus we have shown that the homotopy classes of cuts are classified by the associated system of data. Our task will be now to characterise those systems of data which stem from continuous cuts.

6.3. Propagation of order

The number of possible systems of data seems enormous, since it corresponds to making a choice for each $x \in \mathbf{E}_{\parallel}$. However, we have already seen that for almost all x there is in fact no choice since the corresponding fiber does not intersect any forbidden plane. A further step in that direction is to observe that for a continuous cut, we make in fact only one choice for each forbidden plane. To see this, consider the three-dimensional space defined as the union of the fibers $\pi_{\parallel}^{-1}(x)$ for x belonging to the projection of a forbidden plane. This three-dimensional space contains this forbidden plane which disconnects it so that the trace of the cut in this space (a curve) must stay in one half-space in order not to cross the forbidden plane. Thus the choices in each fiber are correlated and this is best seen in projection onto \mathbf{E}_{\perp} : π_{\perp} maps the forbidden plane onto a straight line and the image of the previous curve must stay on one side of this line. It is now obvious that any system of data compatible with a continuous cut (we shall say just *compatible*) must correspond to the "same" half plane all along the projection on \mathbf{E}_{\parallel} of any forbidden plane, the correlation between half-planes being established through their projection on \mathbf{E}_{\perp} .

The next step is to investigate how the choices are or are not correlated for intersecting forbidden planes. As observed above, there are three cases to

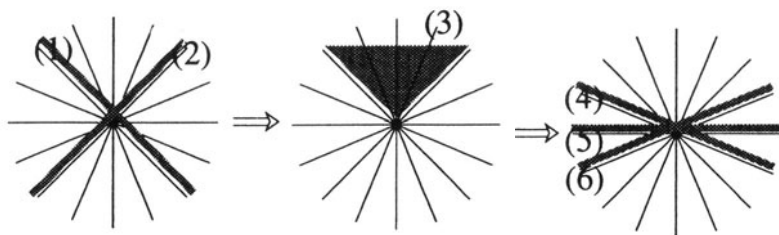


Fig. 14. — Basic mechanism of the propagation of order: the given choices corresponding to the forbidden planes (1) and (2) induce the choice of the sector on the central picture for which the choices of the forbidden planes of type (3) is undetermined but imposes those of type (4), (5) and (6) planes.

consider. In any case, the choice to be made for constructing a system of data is the choice of a angular sector in the fiber, among 4 possibilities in the first case, 8 in the second and 16 in the third.

Here again, there is an obvious constraint: the chosen sector must be contained in all the half-planes selected with respect to the lines intersecting on the considered point. This requirement has no special consequences in the case of pairwise intersection (the sector is then a quadrant which is exactly the intersection of the two half-planes associated to the two lines) but the situation is quite different for the other cases. To understand that point, refer to Fig. 14 and let us suppose that we know what is the half-plane selected along the two lines (1) and (2), as indicated. Then we see that we cannot say anything about the line (3), for which both choices are compatible, but that we can assert what is the half-plane selected “above” the lines (4,5,6), for which only one choice is compatible with the data already known.

This elementary property is in fact the very source of the propagation of the local order which eventually results in the global quasiperiodicity of the structure. The global consequence of this propagation is contained in the following theorem which expresses what are the compatible systems of data, in the sense that they are induced by a continuous cut.

Theorem 1 *The compatible system of data are those for which the closures of the projections of all selected half-planes on E_{\perp} have a non-empty intersection.*

As we shall see, this theorem entails that any tiling fulfilling the matching rules is either quasiperiodic or is the limit of a sequence of quasiperiodic tilings (and such a limit is to a large extent undistinguishable of a strictly quasiperiodic tiling). But let us begin by the proof of the theorem.

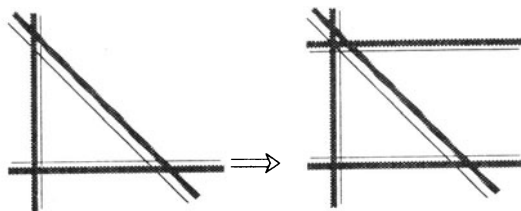


Fig. 15. — To each bad triangle we can attach a bad strip.

6.4. Proof of the theorem

6.4.1. The pushing procedure

Since we want to prove that an infinite family of half-planes have a non empty intersection, we need some tool for reducing the discussion to finite families. Such a tool is conveniently provided by the classical Helly's theorem:

Theorem 2 (Helly) *Consider in \mathbb{R}^n a family \mathcal{F} of convex sets (which must be finite for arbitrary convex sets but may be arbitrary for compact convex sets) such that every finite subfamily of $p \leq n + 1$ sets has a non-empty intersection. Then the whole family \mathcal{F} has a non-empty intersection.*

Since our half planes are not bounded and their family is infinite, we shall need some care when using this theorem. Nevertheless, it allows us to restrict the discussion to pairs and triplets of half planes (in our case $n = 2$). The only case where two half planes may not intersect is when their boundaries are parallel. Let us call *bad strip* such a pair of half planes. Similarly, let us call *bad triangle* a triplet of half planes which do not intersect on the triangle that they define.

Our task is to show that for a compatible system of data, there is no bad strip and no bad triangle. But it is immediate that we can associate a bad strip to any bad triangle: recall that the forbidden planes intersect either by pairs, by quadruplets or by octuplets, and in the first case, the two are orthogonal in both projections on \mathbf{E}_{\parallel} and \mathbf{E}_{\perp} . Thus a bad triangle involves necessarily at least two vertices where 4 or 8 planes intersect, for which we can attach a bad strip (in two or three ways) to the bad triangle, as depicted on Fig. 15.

Finally, it remains to show that there are no bad stripes. Let us suppose that such a bad strip exists. We shall show a contradiction with the continuity of the cut through the construction of a family of forbidden planes about which we know what are the selected half planes. Observe that there are two kinds of bad stripes: those which are parallel to a plane of the type $\varepsilon_1, \varepsilon_2 - \varepsilon_4$ and those which are parallel to a plane of the type $\varepsilon_1 + \varepsilon_2, \varepsilon_3 - \varepsilon_4$. Since the argument is almost the same in both cases, we shall deal in detail only with the first one.

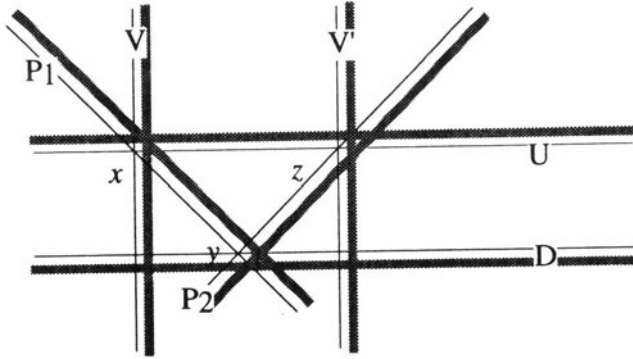


Fig. 16. — The pushing procedure (see text).

For this, consider the Fig. 16, which is drawn in \mathbf{E}_\perp and where the bad strip is horizontal. Let us denote by the same letter U the “upper” plane of the bad strip (parallel to $(\varepsilon_1, \varepsilon_2 - \varepsilon_4)$) and its projection on \mathbf{E}_\perp , and similarly by D the other plane of the strip. We can find a vertical forbidden plane, say V (parallel to $(\varepsilon_3, \varepsilon_2 + \varepsilon_4)$), which intersects the upper line U on a “eightfold” intersection (one half or one quarter of the planes have this property). Let the selected half plane associated to this vertical forbidden plane be the one on the right (which means that the would-be cut would cross each fiber intersecting this vertical plane on the right side of the intersection line).

We can get other vertical forbidden planes “selecting their right side” through the following *pushing procedure* described on Fig. 16. Consider the plane labelled P_1 going through the intersection x and recall that x is the projection on \mathbf{E}_\perp of a body center of \mathbf{Z}^4 : $x = \pi_\perp(\xi)$. In the fiber going through ξ , we find the traces of 8 planes, among which those of U , V and P_1 . As already mentioned, the half plane selected by P_1 must intersect the intersection of the half planes selected by V and U . We see that there is no choice and that the upper-right half plane is selected.

Following P_1 , we arrive to its intersection with D , “above” the point y of \mathbf{E}_\perp . We are either on a fourfold or on a eightfold intersection, and we can consider the plane P_2 . The same argument shows that P_2 selects its lower-right half plane. Along P_2 we find its intersection with U above $z \in \mathbf{E}_\perp$, and through this intersection we can consider the vertical plane V' parallel to V . Then we immediately see that the half plane selected by V' is on the right. Observe at this point that we need to start with a bad strip of *non-zero width* for this argument to be non trivial, and this requires to consider in \mathbf{E}_\perp the closure of the projections of selected half planes, although in each relevant fiber we consider the open selected half-plane, simply because our hypothesis is that the cut never intersects any forbidden plane.

This is the *pushing procedure*. We can iterate it to exhibit a family of forbidden planes parallel to V , of which we know that they select the half plane on the right in each fiber that they meet. Moreover, we have three possible choices for the direction P_1 of the “pusher”, namely those which projects on \mathbf{E}_\perp on e'_4 (this is the direction of plane spanned by $(\varepsilon_4, \varepsilon_1 - \varepsilon_3)$), on $(e'_4 - e'_3)$ $((\varepsilon_4 - \varepsilon_3, \varepsilon_1 + \varepsilon_2))$ and on $e'_1 + e'_4$ $((\varepsilon_1 + \varepsilon_4, \varepsilon_2 + \varepsilon_3))$.

Let us discuss the distribution of this family of planes.

6.4.2. The cone of planes

In order to compute the distances over which we push the vertical plane, let us assume that the distance between U and D (that is, the thickness of the bad strip) is $me'_3 + n(e'_2 + e'_4)$. Then simple geometry shows that the distance between two consecutive planes of the family is:

- $d = 2me'_1 + 2n(e'_2 - e'_4)$ when we push with $(\varepsilon_4, \varepsilon_1 - \varepsilon_3)$
- $d' = (4n - 2m)e'_1 + (2m - 2n)(e'_2 - e'_4)$ for $(\varepsilon_4 - \varepsilon_3, \varepsilon_1 + \varepsilon_2)$
- $d'' = (2m + 4n)e'_1 + (2m + 2n)(e'_2 - e'_4)$ for $(\varepsilon_1 + \varepsilon_4, \varepsilon_2 + \varepsilon_3)$

Now, starting with a given plane V , we can reach any plane sitting at a distance from V which is a linear combination with integer *positive* coefficients of these three distances. Since $d'' = 2d + d'$, we can omit the third one. Observe that the positiveness of the coefficients is very important and corresponds to pushing the planes “on the side they select” in order to flush the would-be cut to infinity.

Thus we find a cone of planes. To describe this cone precisely, let us consider its trace on the plane spanned by $(\varepsilon_1, \varepsilon_2 - \varepsilon_4)$ orthogonal to V (Fig. 17). The whole lattice of forbidden planes parallel to V intersects this plane on a rectangular lattice \mathcal{L} of ratio $\sqrt{2}$. Choosing our V as the origin, consider the two vectors $u = 2m\varepsilon_1 + 2n(\varepsilon_2 - \varepsilon_4)$ and $v = (4n - 2m)\varepsilon_1 + (2m - 2n)(\varepsilon_2 - \varepsilon_4)$ corresponding respectively to d and d' . Our family \mathcal{C} of planes is the trace on the cone defined by the two positive half lines generated by these vectors, of the sublattice of \mathcal{L} which they span.

Observe now that the traces on this plane of \mathbf{E}_\perp and \mathbf{E}_\parallel are respectively the first and the second diagonals of the plane. In fact, we must have on \mathbf{E}_\perp that the projection of $\varepsilon_2 - \varepsilon_4$ is $-\sqrt{2}$ times that of ε_1 , and on \mathbf{E}_\parallel the ratio of the two projections is $+\sqrt{2}$, whence the two diagonals.

The crucial remark is that whatever the thickness of the bad strip is, i.e., whatever the values of m and n are, the edges of this cone fall on the two opposite sides of \mathbf{E}_\perp . To see this, observe that we have measured the thickness upward, so that $m - n\sqrt{2}$ is positive. Then the projection of u and v on \mathbf{E}_\perp are respectively $2(m - n\sqrt{2})e'_1$ and $2((-2n - m) + (m + n)\sqrt{2})e'_1 = 2(\sqrt{2} - 1)(m - n\sqrt{2})e'_1$, and point both to the interior of the cone. On the contrary, the projections of u and v on \mathbf{E}_\parallel are $2(m + n\sqrt{2})e_1$ and $2((-2n - m) - (m + n)\sqrt{2})e_1 = 2(\sqrt{2} + 1)(-m - n\sqrt{2})e_1$, which point on opposite sides.

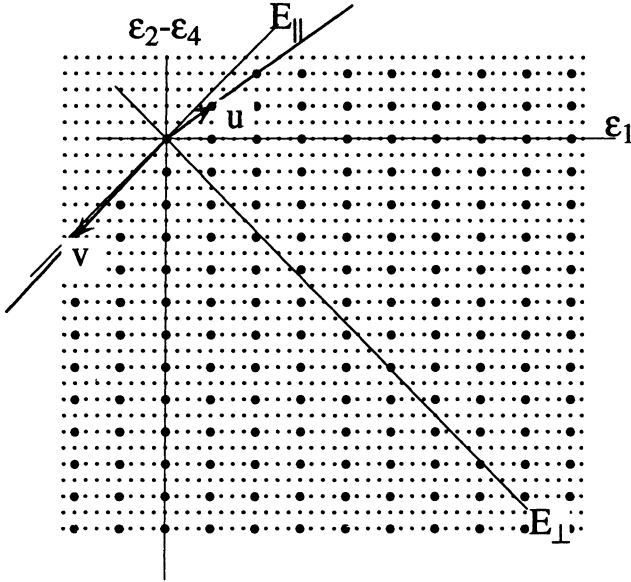


Fig. 17. — The set of planes about which the pushing procedure allows to assert which half plane they select, is the trace of a lattice inside a cone. These planes project *discretely* on E_{\perp} and *densely* on E_{\parallel} .

For the other kind of bad strip, say, parallel to $\varepsilon_1 + \varepsilon_2, \varepsilon_3 - \varepsilon_4$, the drawing of the cone is made in this plane where the relevant forbidden planes form a square lattice. The traces of E_{\perp} and E_{\parallel} are here tilted by $3\pi/4$ with respect to this lattice, but besides this details the main conclusion is the same: the two half lines which bound the cone project one upon the other on E_{\perp} while their projections on E_{\parallel} cover E_{\parallel} .

In other words, the qualitative situation is always that of Fig. 17. We see that the projection of C on E_{\perp} is discrete, although the projections become closer and closer when one goes farther inside the cone. *But the projection of the same family C on E_{\parallel} is everywhere dense*, and this allows us to conclude in the following way:

Consider an generic point x in E_{\parallel} , and the fiber above it, with the trace of the cut. Since the projection of C is everywhere dense in E_{\parallel} , we can find a sequence of lines in this projection converging to a limit going through x . This sequence is the projection of a sequence in C which escape to infinity in the cone, since C is a part of a lattice and does not have any accumulation point. This means that we can find as close to x as we want, a fiber in which the trace of the cut is pushed on the right as far as we want. This is a contradiction with the continuity of the cut and we have shown that a compatible system of data does not admit bad stripes (nor bad triangles as a consequence).

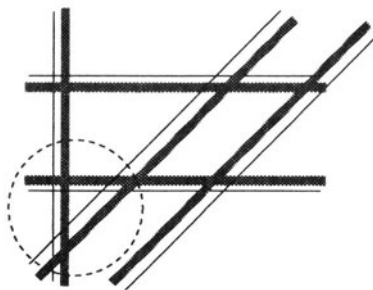


Fig. 18. — Once four forbidden planes have been found which form a parallelogram, the fact that there are no bad stripes nor bad triangles forces the choice for every forbidden plane whose projection on \mathbf{E}_\perp does not cross the parallelogram.

Now we can finish the proof of our theorem. What remains to do is to apply Helly's theorem. For that, consider any forbidden plane and its associated selected half plane in \mathbf{E}_\perp . There exists a parallel plane whose selected half plane is on the opposite side: if that was not the case and since there is no bad stripes, the cut would be entirely at infinity. Thus we have found a strip of finite width such that we know for any forbidden plane parallel to this pair and falling outside the strip, that the associated selected half plane is the one which contains the strip.

Selecting another direction of forbidden planes, we find in the same way another strip which intersects the previous one on a parallelogram. Now we know for any forbidden plane whose projection on \mathbf{E}_\perp does not cross this parallelogram, that the selected half plane contains the parallelogram: otherwise we get a bad triangle, as depicted on Fig. 18.

Finally, we have to discuss the (infinite!) subfamily of forbidden planes whose projection on \mathbf{E}_\perp intersects the parallelogram. But since they project at finite distance of each other, it is no longer necessary to associate to each of them a whole half plane and we can work with *compact* convex sets. Consider in \mathbf{E}_\perp a disc D large enough to contain the parallelogram, and lift it along π_\perp on each fiber. Then consider the intersections of our half planes with the discs instead of the half planes themselves, for all fibers belonging to the subfamily \mathcal{F}' under consideration. Observe that the projection on \mathbf{E}_\perp of these bounded convex sets intersects by pairs and by triplets, otherwise we would get a bad strip or a bad triangle. Then applying Helly's theorem completes the proof of theorem 1.

6.5. Quasiperiodic tilings and "special tilings"

Let us now turn to the consequences of theorem 1 on the quasiperiodicity of well-decorated tilings (Fig. 19). We have just shown that any continuous cut

defines a system of data such that the intersection of the corresponding (closed) half planes is non-empty. Observe first that these intersections are always reduced to a single point. In fact, two distinct points in \mathbf{E}_\perp are always separated by the projection of some forbidden plane, since each lattice of forbidden planes projects on a dense set of lines. Thus two distinct points correspond to two different systems of data. Then the conclusion depends on whether this point x does or does not belong to the projection of some forbidden plane.

The simple case is when the point x falls in the complementary of the projection of the forbidden planes. Then we can consider the plane cut parallel to \mathbf{E}_\parallel and going through x : it is a regular cut which intersect the atomic surfaces on their interiors and **defines a quasiperiodic tiling**. This is the generic case. Observe that in this case, the point x is as well the intersection of all the projections of the *open* selected half-planes, in such a way that we have a one-to-one correspondence between quasiperiodic tilings and connected components of the complementary of the projection on \mathbf{E}_\perp of the forbidden planes.

But this family of quasiperiodic tilings does not exhaust the set of all well-decorated tilings, and we have to consider the cases where the point x falls on the projection of one or several forbidden planes. We shall call *special* the tilings of this kind. For the sake of simplicity, let us first suppose that x belongs to the projection D of one forbidden plane P only. Such a point x corresponds to two distinct systems of data, differing by the choice relative to the forbidden plane P . It is clearly impossible to choose a “perfectly” plane cut to define the corresponding tilings: the only possible plane cut goes through P and we have to distort it (as slightly as we want) on one side or on the other, above the projection of P on \mathbf{E}_\parallel .

These well-decorated special tilings, which are not as “strongly” quasiperiodic as the previous ones, may be conveniently described in our case as limits of quasiperiodic tilings in the following way:

Consider in \mathbf{E}_\perp a smooth arc parameterised by the interval $[0, 1]$, transversal to the projections of all forbidden planes and such that the image of 0 belongs to the projection D of a forbidden plane. Consider on this arc a sequence of points x_n converging to the image x of 0 and such that no point in this sequence falls on the projection of a forbidden plane. Then each of these points x_n corresponds to a well-behaved quasiperiodic tiling \mathcal{T}_n . We define the limit tiling \mathcal{T} corresponding to x as a simple limit: a vertex belongs to \mathcal{T} if and only if it belongs to \mathcal{T}_n for infinitely many n (observe that we have constrained the sequence x_n to belong to a smooth arc in order to avoid pathologies such that sequences oscillating or spiralling towards their limit).

Because of the local constancy of local patterns with respect to shifts of the cut along \mathbf{E}_\perp , it is quite obvious that the limit obtained in this way is a well-decorated tiling (any *bounded* region in \mathcal{T} occurs in infinitely many \mathcal{T}_n). It follows in particular that these special tilings have no particular *local* property. But they do have a special global property, namely they contain a finite number of *infinite worms*. For instance, if the limit x belongs to the projection D of only one forbidden plane P , then we find in the limit tiling only

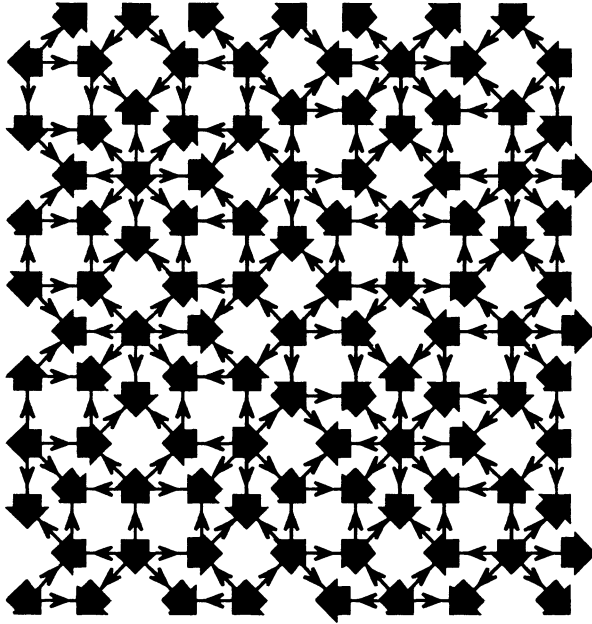


Fig. 19. — A sample of octagonal tiling, decorated with Ammann rules.

one infinite worm (whose axis is the projection of P on E_{\parallel}) and if we consider now another sequence x'_n converging to x from the other side of D , we find in the corresponding limit tiling the “flipped” version of the worm. Of course, the superimposition of these two limits is just the trace of the oblique tiling in the singular cut defined by x . The axis of the worm is almost a symmetry axis of the tiling, which is broken only along the worm: if P belongs to the second kind of forbidden planes, the two limit tilings share the same sets of vertices and only the vertex decoration along the worm is “flipped” between the limits. If P belongs to the first kind of forbidden planes, then the limit tiling is defined by a plane cut which goes through the *boundary* of a family of atomic surfaces, and the taking of a limit is a consistent way to select half of the concerned atomic surfaces.

If now the intersection x of the closure of the projection of all the selected half-planes belongs to several images of forbidden planes, we must be careful not to “pinch” the cut between forbidden planes upon flipping worms. Recall that, although we have taken the closure of the projection of the selected half-planes in order to develop our pushing argument, the cut is not allowed to intersect the forbidden planes. Observe first that we have to study only a *finite* number of different tilings. In fact, such an x is either the intersection of two,

four or eight projections of forbidden planes, and there is only a finite number of orbits for such a point under the projection of the 4-dimensional lattice. But recall that two tilings whose associated plane cuts are mapped on each other by a translation belonging to the high-dimensional lattice are just the same tiling, up to a global translation which is the projection on \mathbf{E}_{\parallel} of the high-dimensional translation.

Consider a special tiling for which the point x falls on the intersection of only two projections of forbidden planes. Let ξ be the intersection of these planes (we know that ξ is a face center), and consider the fiber parallel to \mathbf{E}_{\perp} going through ξ . We see that we can flip freely each of the worms associated to the two forbidden planes. In fact, each choice of passing the cut on one side or the other of each forbidden plane correspond to a quadrant in this fiber, and the cut is never pinched. But the situation is quite different when x belongs to the intersection of four or eight forbidden planes (then ξ is respectively a vertex or a body center of the 4-dimensional lattice). Defining one of the corresponding special tilings as a limit, the traces of the associated sequence of cuts in the fiber going through ξ is a sequence of points converging to the intersection of the traces of the forbidden planes. This sequence of points is contained in one of the eight or sixteen sectors defined in this fiber and the tiling of the worms in the limit tiling is prescribed by this sector. We get complete worms only for the forbidden planes bounding this sector, and we can flip one of them. This operation just yields the limit tiling obtained in a sector adjacent to the initial one. Finally, we see that we access only eight different special tilings associated to fourfold intersections and sixteen in the case of eightfold intersections.

Let us now explain in which sense these special tilings are “less” quasiperiodic than regular ones. Recall that in the standard computation of the Fourier transform, we take the multiplicative product of the Lebesgue measure carried by the plane cut and of the measure carried by the atomic surfaces. But such a multiplicative product of generalised functions exists only under a transversality condition which is precisely violated when the cut intersects the atomic surface on its boundary. Thus the computation breaks down and *this* notion of quasiperiodicity does not apply to the special tilings involving coming on the projection of forbidden planes of the first kind. Observe on the other hand that nothing dramatic happens to the special tilings: since the ambiguous vertices (those on the worm) constitute a vanishingly small fraction of the set of vertices of the tiling, the statistical notions such as autocorrelation functions, which define the physically relevant quantities, are exactly the same for special tilings and for regular tilings.

7. GENERALISED AMMANN TILINGS

7.1. Definitions

As already explained, we need two sets of forbidden planes in order to implement the Ammann decorations of the octagonal tilings: the first set corresponds to the edge part of the decoration, and the second set to the vertex part. We shall now study what happens when one keeps only one of these two sets, and the associated decoration. As we shall see, the corresponding decorated tilings are still highly ordered: they are either quasiperiodic or periodic, up to some discrepancies that we shall explain.

We shall call generalised Ammann tilings of the first kind those for which we keep only the edge decoration to define the matching rule, and accordingly generalised tilings of the second kind those with only the vertex decoration. Let us first discuss which symmetry properties may remain for the generalised tilings, provided that they are ordered enough to keep some symmetry.

7.2. Symmetry considerations

Recall that the octagonal group acting in the plane is a Coxeter group generated by two reflections, and we may take for instance as generating mirrors of this action in \mathbf{E}_{\parallel} the two lines spanned respectively by e_1 and $e_1 + e_2$. This group contains two subgroups isomorphic to the symmetry group of the square, which is still a Coxeter group. We may take as mirrors generating the first subgroup the two lines spanned by e_1 and e_2 , and as mirrors generating the second one those spanned by $e_1 + e_2$ and $e_2 + e_3$. We have a similar construction in \mathbf{E}_{\perp} .

These two subgroups are linked with the two kinds of forbidden planes in the following way: recall that we have lifted in \mathbb{R}^4 the action of the octagonal group, so that we have in particular an action of the two subgroups, and we know how to transform any 2-dimensional plane embedded in \mathbb{R}^4 under these actions: in other words, we have an action of the octagonal group and of its subgroups on the Grassmannian manifold \mathcal{G}_2^4 of the 2-dimensional planes of \mathbb{R}^4 .

Then it is easy to see that the planes simultaneously non-transversal to the four directions of the first set of forbidden planes are invariant under the action of the first subgroup, and their set is a one-dimensional smooth submanifold \mathcal{S}_1 of \mathcal{G}_2^4 . We have a similar result for the second set of forbidden planes and our second subgroup, which yields another smooth submanifold \mathcal{S}_2 of \mathcal{G}_2^4 . The two curves \mathcal{S}_1 and \mathcal{S}_2 intersect on two points in \mathcal{G}_2^4 . The corresponding planes, which are invariant through both subgroups, are invariant through the whole octagonal group and are obviously our \mathbf{E}_{\parallel} and \mathbf{E}_{\perp} .

Finally, the canonical cut construction of the octagonal tilings generalises as follows: setting once for all \mathbf{E}_{\perp} as the plane carrying the atomic surface, we consider a *plane* cut non intersecting the first set of forbidden planes. The direction of such a plane is surely non-transversal to the four directions of for-

bidden planes, so that the direction of the cut belongs to \mathcal{S}_1 . Setting as atomic surface the projection of the unit hypercube on \mathbf{E}_\perp along the cut, we take the intersections of the cut with the lattice of these atomic surfaces and project these points on \mathbf{E}_\parallel along \mathbf{E}_\perp to get the vertices of a generalised Ammann tilings of the first kind. It is made of the same rhombi and squares as the octagonal tiling and possesses the symmetry of the square to the same extent that the Ammann tilings are octagonal. Also, it admits the edge decoration by its very construction. We set an obviously similar construction for the generalised tilings of the second kind.

A remarkable property of both \mathcal{S}_1 and \mathcal{S}_2 is that these two curves contains infinitely many points corresponding to planes with a completely rational direction. For such a direction, the cut construction yields periodic tilings. Otherwise, we get quasiperiodic tilings.

However, we are concerned by the converse problem: we would like to show that any tiling admitting the edge decoration alone (or the vertex decoration alone) is (up to some discrepancies for special tilings) a periodic or quasiperiodic tiling. For the sake of clarity, we shall work out the construction for the case of the generalised Ammann tilings of the first kind (edge decoration). Also, from now on, we shall consider as forbidden planes the first family only.

7.3. Setting the method

This problem is clearly more difficult than for the octagonal case. In that latter case, we had for symmetry reasons only one candidate for the direction of the plane cut we were looking for inside the homotopy class of cuts defining a given tiling: namely the direction of \mathbf{E}_\parallel . This is no longer the case, since any direction belonging to the curve \mathcal{S}_1 of the Grassmannian manifold is a possible candidate, and this forces us to refine our method.

We shall still describe a general cut by its intersections with fibers parallel to \mathbf{E}_\perp . Since the generalised tilings are still built by projecting the selected points on \mathbf{E}_\parallel , we may as previously limit our considerations to cuts everywhere transversal to \mathbf{E}_\perp , (in order to get a one-to-one projection of the cut on \mathbf{E}_\parallel along \mathbf{E}_\perp) so that the cut yields exactly one intersection in each fiber. Then, since \mathbf{E}_\perp is non-transversal to the directions of the forbidden planes, we define the same notion of system of data as in the octagonal case: nothing is changed from that point of view.

Our problem is again to show that a compatible system of data is associated to a homotopy class of cuts which contains a plane. In the octagonal case, we mapped the forbidden planes on \mathbf{E}_\perp along \mathbf{E}_\parallel , which was the only direction to be considered, and developed the globalisation argument in \mathbf{E}_\perp . This is the point we have to generalise in order to take into account that we have now a whole one-parameter family \mathcal{S}_1 of possible plane directions for the cut.

Let us consider the 3-dimensional space $\mathcal{E}_1 = \mathbf{E}_\perp \times \mathcal{L}_1$, where $\mathcal{L}_1 = \mathbb{R}$ is a local chart of \mathcal{S}_1 , which we define as follows: take anyone of the four directions of forbidden planes and consider in this plane the traces of the planes belonging

to \mathcal{S}_1 . On account of the non-transversality, these traces are straight lines and we take as coordinate along \mathcal{S}_1 the tangent of the angle φ between the trace of \mathbf{E}_{\parallel} and that of the given plane; because of the symmetry, this definition does not depend on the chosen direction of forbidden planes (up to a sign). We restrict the domain \mathcal{S}_1° of the chart to angles $\varphi \in [-\pi/4, +\pi/4]$ because for larger angles we get overlapping tiles. It is easy to see from elementary geometry that when we vary φ , the projections on \mathbf{E}_{\perp} of the basis vectors keep the same relative angles, the length of the projections of ε_1 (resp. ε_2) remains equal to that of ε_3 (resp. ε_4), and the ratio of these lengths varies like $\tan(\varphi + \pi/4)$. For $\varphi = \pm\pi/4$, one or the other pair yields a null projection, so that the atomic surface become a square and the corresponding tilings are simple square tilings built with one or the other of our square tiles.

The 3-dimensional space \mathcal{E}_1 is to be considered as a stack of copies Φ_φ of \mathbf{E}_{\perp} , each attached to the direction in \mathcal{S}_1 along which we project \mathbb{R}^4 on \mathbf{E}_{\perp} : the fiber Φ_0 above $\varphi = 0$ is the one for which \mathbb{R}^4 is projected along \mathbf{E}_{\parallel} , and is just \mathbf{E}_{\perp} as we have used it when dealing with the octagonal case.

Now, we define the map

$$\mathcal{F}_1 : \mathbb{R}^4 \times \mathcal{S}_1^\circ \mapsto \mathcal{E}_1$$

which send a pair $(\xi, \varphi) \in \mathbb{R}^4 \times \mathcal{S}_1^\circ$ on the projection of ξ on \mathbf{E}_{\perp} along the direction designated by φ , so that the image is a point in the fiber Φ_φ . Then, due to the non-transversality of the forbidden planes to any plane in \mathcal{S}_1 , the image by \mathcal{F}_1 of any forbidden plane P is a straight line in each fiber Φ_φ , and due to the choice of the parameterisation $\tan(\varphi)$ along \mathcal{L}_1 , these lines align along a plane in \mathcal{E}_1 when φ describes \mathcal{S}_1° . Thus, the image $\mathbf{P} = \mathcal{F}_1(P, \mathcal{S}_1^\circ)$ is a two dimensional plane in \mathcal{E}_1 .

Let us describe briefly the geometry of this collection of planes. Consider first the images of two parallel forbidden planes: their traces in each fiber Φ_φ are parallel lines, but due to the irrational direction of \mathbf{E}_{\perp} , the distance between these lines changes with the projecting direction φ , so that there are no parallel planes in the collection. Second, observe that two planes \mathbf{P} and \mathbf{P}' intersect along a line contained in a fiber Φ_φ if and only if, first, they come from parallel forbidden planes, and second, the direction φ corresponds to a rational plane. Then we find a whole infinite family of planes intersecting on the same line, coming from an affine sublattice of parallel forbidden planes. Moreover, in such a fiber Φ_φ where φ is the coordinate of a rational plane, we find a whole lattice of parallel lines on which intersect the images of sublattices of forbidden planes: in these fibers, the traces of our planes build a periodic decomposition of the fiber. On the contrary, the fibers corresponding to irrational directions in \mathcal{S}_1 are densely filled by the traces of the planes, in the way we are used to for the projection on \mathbf{E}_{\perp} along \mathbf{E}_{\parallel} , which is now found as Φ_0 .

On the other hand, consider the intersection \mathbf{D} of two planes \mathbf{P} and \mathbf{P}' coming from non-parallel forbidden planes P and P' . Its trace on each fiber Φ_φ is the intersection of the corresponding projections of P and P' on \mathbf{E}_{\perp} . But since non-parallel forbidden planes are transversal, they actually intersect

in \mathbb{R}^4 and this trace is the projection of the intersection $\xi = P \cap P'$. Thus the whole line \mathbf{D} is the image $\mathcal{F}_1(\xi, \mathcal{S}_1^\circ)$. In particular, the discussion of section 6.1 applies and we see that such a line \mathbf{D} is either the intersection of two planes \mathbf{P} and \mathbf{P}' (if ξ is a face center) or of four such planes if ξ is a body center. Finally, observe that, once again because the direction of \mathbf{E}_\perp is irrational, for no pair of lines $(\mathbf{D}, \mathbf{D}')$ are parallel.

7.3.1. Systems of data in \mathcal{E}_1

Our next task is to translate in the space \mathcal{E}_1 the notion of system of data, since the globalisation procedure using Helly's theorem will take place in \mathcal{E}_1 . Let us return in \mathbb{R}^4 considered as usual as the trivial fiber bundle $\mathbf{E}_\perp \times \mathbf{E}_\parallel$, in which we describe a cut by considering for each $x \in \mathbf{E}_\parallel$ its trace on the corresponding fiber. Recall that for non-transversality reasons the forbidden planes disconnect the fibers that they intersect, so that we characterise the homotopy class of a cut by specifying the relevant connected component in each fiber. Recall also that the choice made at one point $x \in \mathbf{E}_\parallel$ relatively to one forbidden plane is forced (by the non-intersection condition) all along the projection of this forbidden plane on \mathbf{E}_\parallel , so that the choice is in fact attached to each forbidden plane rather than to points of its projection on \mathbf{E}_\parallel . Now we can translate such a choice in \mathcal{E}_1 simply by observing that it is quite independent of the direction φ of the projection: we copy this choice in each fiber Φ_φ of \mathcal{E}_1 and this amounts to select one of the two half-spaces defined in \mathcal{E}_1 by the image of the forbidden plane (observe that the domain \mathcal{S}_1° of the chart \mathcal{L}_1 on \mathcal{S}_1 is small enough to allow this procedure).

The strategy to prove that the edge decoration is sufficient to enforce periodic or quasiperiodic order (up to something) will as in the octagonal case consist in showing that a system of data is compatible with its definition by a continuous cut if and only if the associated half-spaces selected in \mathcal{E}_1 have a non-empty intersection.

We shall prove the following:

Theorem 3 *The compatible systems of data are those for which the closures of all selected half-spaces in \mathcal{E}_1 have a non-empty intersection.*

7.4. Reduction to “bad prisms”

In view of the application of Helly's theorem in \mathcal{E}_1 , we have to show that, for a system of data defined by a continuous cut, any pair, triplet and quadruplet (\mathcal{E}_1 is 3-dimensional!) of selected half-spaces in \mathcal{E}_1 has a non-empty intersection. Observe first that since there is no pair of parallel planes, the intersection of two selected half spaces is never empty. Next, it is immediate that in order for a triplet of half-spaces to have an empty intersection, the pairwise intersections of the corresponding planes must be three parallel lines, in which case each of them is contained in a fiber Φ_φ and the three planes come from parallel forbidden planes. We shall refer to this configuration as a “bad prism”.

Now we want to show that to any “bad quadruplet” of half-spaces, we can attach a bad prism (just as we have attached a bad strip to any bad triangle in section 6.4.1). There are several configurations to study and we shall just sketch the arguments.

Let us classify the possible configurations according to the number of parallel lines among the intersections of our four planes. If we have four parallel lines, then the configuration is a prism with a quadrangular basis and any triplet of planes among the four defines a bad prism. If we have three parallel lines, then the configuration is a bad prism crossed by the fourth plane and we simply retain the bad prism. The situation with only two parallel lines just does not exist, so that it remains to examine tetrahedral configurations.

To deal with them, we use two facts: first, considering any edge of the tetrahedron which is not contained in a fiber Φ_φ , we know that it comes from an intersection of forbidden planes. Depending on the intersection and of the half-planes selected in the corresponding fiber of \mathbb{R}^4 , we may be able to find one or several other forbidden planes going through the same intersection about which we know which are the selected half-planes (see Fig. 14). These planes are mapped in \mathcal{E}_1 onto planes containing the given edge. Second, considering a “bad tetrahedron” and any other plane crossing it, we can build another bad tetrahedron bounded by this last plane (whatever the selected side is). This allows to get rid of some special configurations, and the inspection of all possible cases shows that it is always possible to associate a bad prism to a bad tetrahedron.

7.5. Proof of the theorem

The reduction to bad prisms allows us to work out the proof in a planar section of \mathcal{E}_1 . Suppose for instance that the direction of forbidden planes involved in the bad prism is $(\varepsilon_1, \varepsilon_2 - \varepsilon_4)$ and consider the plane in \mathcal{E}_1 spanned by \mathcal{L}_1 and the direction e'_3 (or $e'_2 + e'_4$) in \mathbf{E}_\perp . In this plane, the trace (and the projection) of the bad prism is the bad triangle depicted on Fig. 20. The vertices of the triangle project on \mathcal{L}_1 on $\varphi_1, \varphi_2, \varphi_3$ such that $\varphi_1 < \varphi_2 < \varphi_3$ (inequalities are strict because there is no “vertical” plane \mathbf{P} in \mathcal{E}_1 : such a plane would be the image of a forbidden plane located at infinity in \mathbb{R}^4). Let us choose a $\varphi \in]\varphi_1, \varphi_2[$ (or, equivalently $\varphi \in]\varphi_2, \varphi_3[$) corresponding to an irrational plane (in order to avoid superimposition of projections of forbidden planes) and consider the situation in the fiber Φ_φ (Fig. 21): whatever the choice of φ is, the forbidden planes whose images in \mathcal{E}_1 build the bad prism project on two bad stripes (P_1, P_2) and (P_3, P_2) to which we can apply our pushing procedure.

This is the key of the proof: in the octagonal case, we made use of only one bad strip, but we had two rationally independent distances to push a forbidden plane along it, using as the “pusher” two forbidden planes of the two different kinds. Now, we have only the four forbidden planes of the first kind, so that we have only one choice for the “pusher” and the whole procedure generates only a

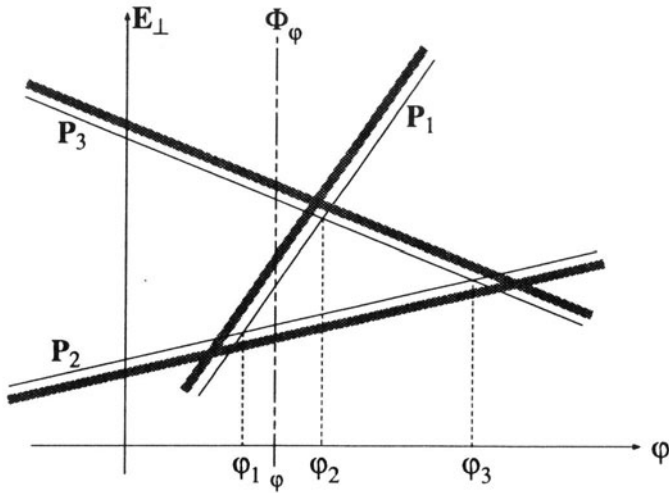


Fig. 20. — The traces of the planes P_1 , P_2 and P_3 forming a bad prism define a bad triangle in the relevant plane of \mathcal{E}_1 .

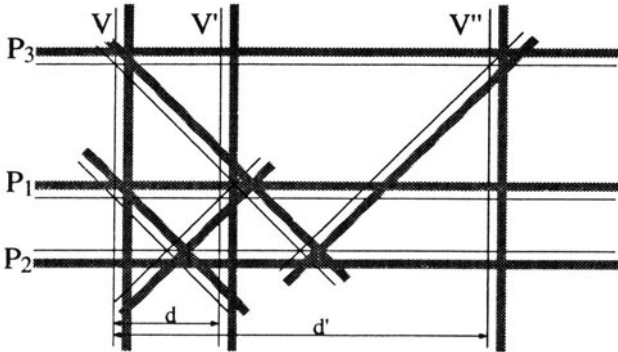


Fig. 21. — The trace of the bad prism in any fiber Φ_φ with $\varphi_1 < \varphi < \varphi_3$ contains two bad stripes, so that the pushing procedure allow to push the plane V on two distances d and d' .

half one-parameter sublattice of forbidden planes “about which we know which half-plane is selected”. Recall that this does not result in any contradiction, for which we need a suitably oriented cone of planes. This difficulty is solved in the present framework by the occurrence of two bad stripes in the construction, which together allow to recover a whole cone of planes.

In fact, there is nothing more to say about the pushing procedure. The only point to be studied is the relative position of the cone of planes with respect

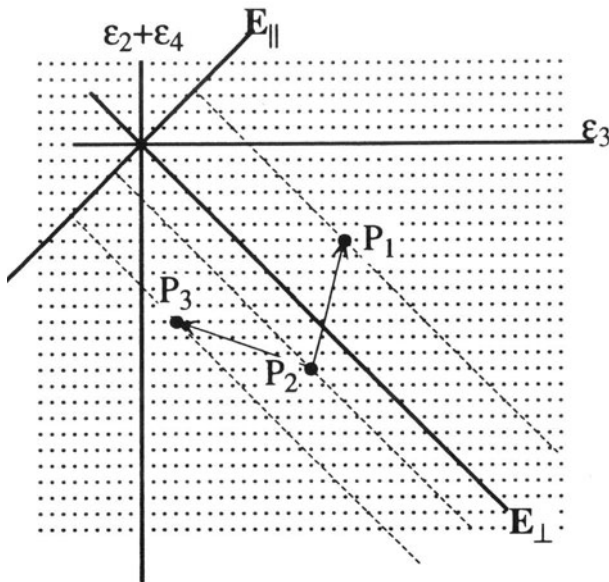


Fig. 22. — The three forbidden planes P_1 , P_2 and P_3 are located in \mathbb{R}^4 in positions corresponding to the slope of their images P_1 , P_2 and P_3 in \mathcal{E}_1 , in such a way that in projection on \mathbf{E}_\parallel , P_2 falls between P_1 and P_3 .

to the pair $(\mathbf{E}_\perp, \mathbf{E}_\parallel)$. For this, let us first consider simultaneously the two figures Fig. 20 and Fig. 22, which represents through its trace in the plane $(\epsilon_3, \epsilon_2 + \epsilon_4) \subset \mathbb{R}^4$ the lattice of forbidden planes $(\epsilon_1, \epsilon_2 - \epsilon_4)$ among which are the three planes P_1, P_2, P_3 forming our bad prism.

In order to correlate the lines in Fig. 20 and the corresponding points in Fig. 22, observe that *the slope of the lines* in the first figure corresponds to *the distance to \mathbf{E}_\perp* of the corresponding vertices in the second one: the vertices whose projection on \mathbf{E}_\perp moves quickly with the direction φ of the projection (and which corresponds to large slopes on Fig. 20) are those which are far from \mathbf{E}_\perp on Fig. 22. Thus we see that the projections on \mathbf{E}_\parallel along \mathbf{E}_\perp of the vertices P_1, P_2, P_3 are such that the projection of P_2 lies *between* those of P_1 and P_3 .

This piece of information will be sufficient for us. Let us return to Fig. 16 to observe that, since our “pusher” makes an angle of $\pi/4$ with both the pushed plane V and the direction of the bad strip, the components of the displacement in the coordinates $(\epsilon_1, \epsilon_2 - \epsilon_4)$ are just twice the components of the width of the bad strip in the coordinates $(\epsilon_3, \epsilon_2 + \epsilon_4)$, so that the basis of our cone of planes is obtained by copying in the plane $(\epsilon_1, \epsilon_2 - \epsilon_4)$ of Fig. 17 the two vectors $(P_1 - P_2)$ and $(P_3 - P_2)$ read on Fig. 22, and doubling them. Then the remark above entails that this cone contains \mathbf{E}_\perp , and thus that the vertices it contains project densely on \mathbf{E}_\parallel , which was the point to be proved.

The end of the proof runs exactly like in the octagonal case and does not need details: the pushing procedure exhibits a contradiction with the continuity of the cut, so that a compatible system of data does not have any bad prism, and applying Helly's theorem then concludes the proof of theorem 3.

7.6. Order in generalised Ammann tilings of the first kind

Let us now turn to the consequences of this theorem for the ordering of the well-decorated tilings. As for the octagonal case, we shall distinguish between the generic situation and the special tilings.

The generic case is such that the intersection of the (closed) half-spaces defined by the system of data does not intersect any image \mathbf{P} of a forbidden plane, so that it is also the intersection of the corresponding family of *open* half-spaces. Such an intersection is a connected component of the complementary in \mathcal{E}_1 of the images $\mathbf{P} = \mathcal{F}_1(P, \mathcal{S}_1)$ of all the forbidden planes P . Let us describe these connected components. The main point is that all of them are entirely contained in a single fiber Φ_φ . In fact, the collection of planes \mathbf{P} contains planes as close to the fibers as we want (coming from forbidden planes as far as we want in \mathbb{R}^4) so that any two points in different fibers can be separated by such a plane and do not belong to the same connected component. Now there are two cases: in fibers corresponding to irrational directions, the traces of the planes \mathbf{P} are dense and the connected components are reduced to single points. In fibers corresponding to rational directions, the planes \mathbf{P} fall on four discrete grids which generate a periodic decomposition of the fiber (which we refrain from calling a tiling for the sake of clarity). In both cases, the system of data may be defined by a plane cut parallel to the plane designated by the coordinate φ of the fiber Φ_φ which contains the intersection, and going through the corresponding point of \mathbf{E}_\perp (in the irrational case) or anywhere in the interior of the corresponding cell (in the rational case). **The corresponding generalised Ammann tilings are respectively quasiperiodic and periodic**, as illustrated on Fig. 23.

Concerning the special tilings, it is still true that they correspond to intersections of closed half-spaces entirely contained in a single fiber Φ_φ , but now the situation is rather different when φ corresponds to a rational direction and when it corresponds to an irrational one.

If φ corresponds to an irrational direction, the discussion of section 6.5 applies completely: we find a finite number of infinite worms, which we can flip according to a non-pinching restriction. Averaged physical quantities do not distinguish between quasiperiodic and special tilings corresponding to the same φ .

The family of special tilings is paradoxically much more larger in the periodic case, where φ correspond to a rational direction of the cut. As mentioned above the forbidden planes project on such a fiber Φ_φ on the boundaries of a periodic cellular decomposition of the plane, in which each cell corresponds to a periodic tiling. Of course, two cells mapped on each other by the translation group of

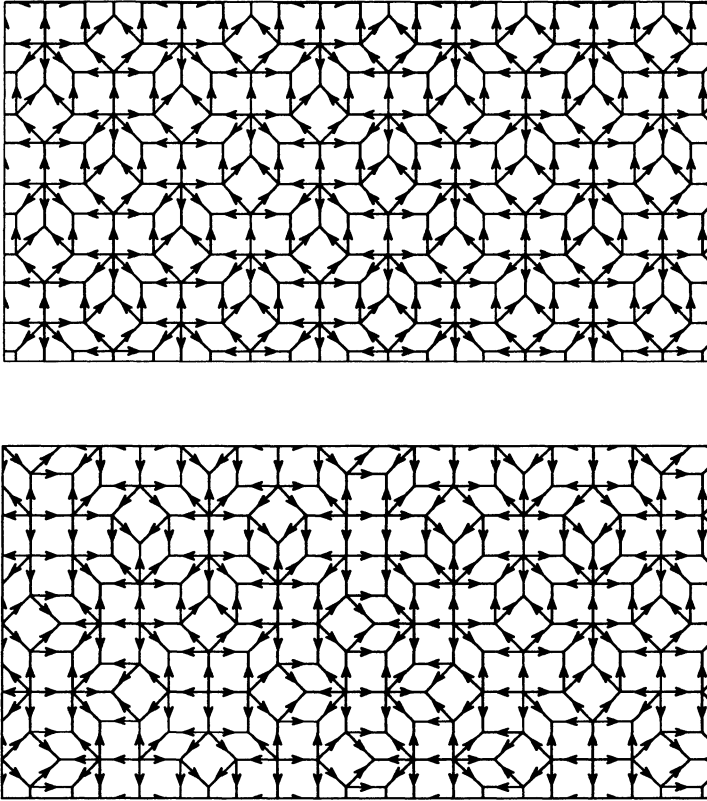


Fig. 23. — Two examples of generalised Ammann tilings of the first kind: (top) periodic tiling corresponding to $\varphi = \arctan(3 - 2\sqrt{2})$; (bottom) quasiperiodic tiling corresponding to $\varphi = 15^\circ$.

the periodic decomposition of Φ_φ define the same tiling, so that we find in fact finitely many different periodic tilings associated to the angle φ . Let us consider the special tilings associated to an edge of a cell: this line is the image of a whole sublattice of parallel forbidden planes. They are (with one exception to be dealt with below) associated with a whole lattice of worms which we can flip independently. If we start from a regular tiling associated with the interior of a cell, and we flip *all* the worms associated with a given edge of this cell, we end of course with the regular tiling associated with the adjacent cell. But we can flip any arbitrary subset of worms, still keeping a well-decorated tiling.

If now we come on a vertex of a cell, there are again two cases: if this point is the image of a face center (in which case this vertex is the intersection of

two orthogonal lines and belongs to four cells), then we find two perpendicular lattices of worms which do not “interact”, in the sense that here again we can flip any arbitrary subset of both family of worms, still keeping a correct decoration. When the vertex is the projection of a body center, the situation is much more complicated: let w and w' be the two families of relevant worms, which form an angle of $\pi/4$. It is obviously possible to flip an arbitrary subset of *either* w or w' , but let us try to combine flips from the two families: let us flip first a worm from w . This operation breaks all the worms of w' on their intersections with the flipped one and produces pieces of worms of a third direction w'' , but these are broken on their intersections with all the other worms of w . Thus it seems that when one flips one worm, only the worms parallel to this one remain complete. It is unclear in this case whether it is possible or not to find well decorated special tilings besides the above-mentioned ones.

Finally, let us say a word about the strangest tiling of all, which is obtained for $\varphi = \pm\pi/4$ and has no worms at all: it is the regular square tiling! Without insisting, let us mention that it is possible to produce a well decorated special tiling associated to it by taking a limit of tiling along a sequence with $\varphi_n \rightarrow \pi/4$, depicted on Fig. 24.

As a conclusion on this section, let us remark that the notion of matching rules (even strong like these) seems not to fit so easily with the notion of (quasi)periodicity. Everything goes smoothly as long as regular tilings are concerned. But we cannot escape the special tilings (recall that they are locally the same as regular ones, so that no *local* matching rule can reject them), and in the periodic case, special tilings may differ from a periodic one for a *finite* fraction of their vertices, so that physical averaged quantities may reveal that they are less ordered than periodic ones.

7.7. Generalised Ammann tilings of the second kind: an example of weak rules

One can develop the same theory with the vertex decoration and the second family of forbidden planes. We shall not repeat the arguments, leaving them as an exercise to the reader. Let us only set up the framework.

We need now an auxiliary space $\mathcal{E}_2 = \mathbf{E}_\perp \times \mathcal{L}_2$, where \mathcal{L}_2 is a local chart on \mathcal{S}_2 defined in a quite similar way as \mathcal{L}_1 : considering the traces of the planes belonging to \mathcal{S}_2 on the direction of any forbidden plane of the second kind, we observe that these traces are lines so that we define the coordinate ψ of a plane in \mathcal{S}_2 as the angle between \mathbf{E}_\parallel and the given plane of \mathcal{S}_2 , and we set on \mathcal{L}_2 the parameter $\tan(\psi)$. Notice that now the domain \mathcal{S}_2° of the chart is limited to $\psi \in [-\pi/8, +\pi/8]$, in order to avoid overlapping tiles. Here again, simple geometry shows that when we vary ψ , the lengths of the projections on \mathbf{E}_\perp of the basis vectors remain the same, but the pair $(\varepsilon_2, \varepsilon_4)$ rotates relatively to the pair $(\varepsilon_1, \varepsilon_3)$ of twice the variation of ψ . For the extremal values $\psi = \pm\pi/8$, the two pairs become collinear and we get as atomic surface a square whose edges

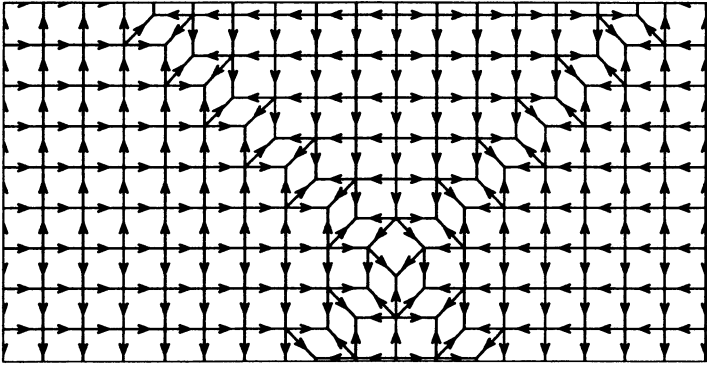


Fig. 24. — Special tiling associated to the regular square tiling. It is obtained by taking a limit for $\varphi \rightarrow \pi/4$, such that the limit cut goes through a vertex of the periodic decomposition of the fiber $\Phi_{\pi/4}$. If the limit cut goes only through an edge, one of the worm is sent to infinity, and of course if the limit cut goes through the interior of a cell, we get the regular square tiling.

are the sum of the projections of two basis vectors. The existence domains of two rhombi over the four vanish, so that we get tilings made of the two squares and two of the rhombi. These tilings are periodic.

We show on Fig. 25 some examples of generalised Ammann tilings of the second kind.

The important point is that the matching rules thus obtained are only **weak rules**, in the sense of Levitov ([1]).

To elucidate this point, let us return to the very beginning of our theory (section 4.3). By its very definition, the forbidden set touches the atomic surfaces on their boundaries. But the forbidden planes of the first kind on which we have retracted this forbidden set no longer intersect the atomic surfaces. However, we have completely forgotten about atomic surfaces during the development of the theory, dealing only with the forbidden planes. In fact, our rules for the octagonal tilings and for the generalised Ammann tilings of the first kind are strong rules only if the following property holds: it is not possible to distort a cut so as to switch an intersection point from a given atomic surface to a neighbouring one, without intersecting a forbidden plane.

To verify that this is the case for the first family of forbidden planes and not for the second, the simplest way is to refer to the “closeness property” of the atomic surfaces. This property plays an important role in the geometry of quasicrystals ([28],[19]), but we do not need to explain it in the large and we shall only make use of the following simple argument:

Consider the lattice of octagonal atomic surfaces, appended by their centers

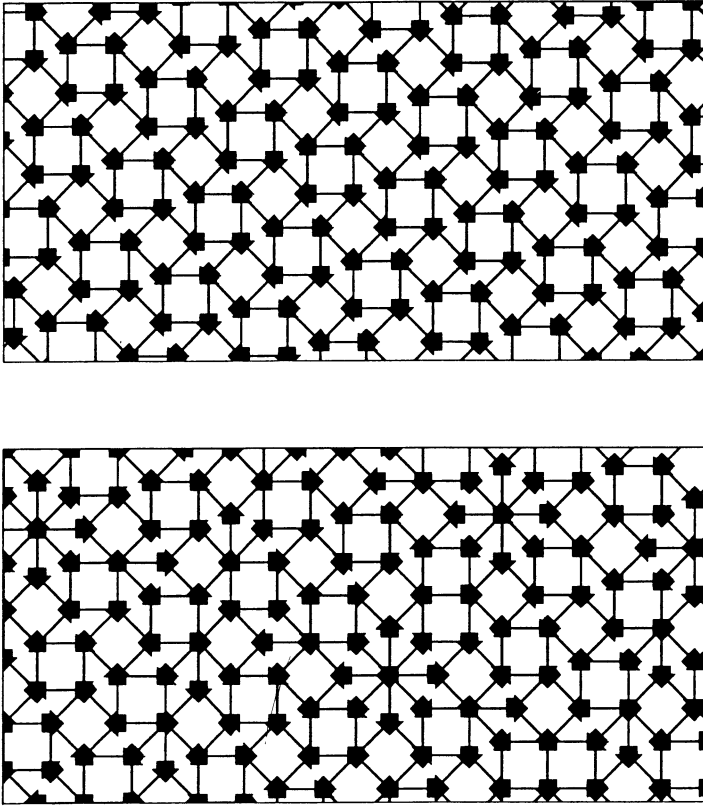


Fig. 25. — Two examples of generalised Ammann tilings of the second kind: top: the periodic tiling obtained for $\psi = \pi/8$; bottom: a quasiperiodic tiling corresponding to $\psi = 10^\circ$.

to the vertices of the four dimensional simple lattice \mathbb{Z}^4 . It is possible to “complete” these atomic octagons in order to get a manifold without boundary. This is done in two steps. The first one consists in gluing along the edges of the octagons four sets of rectangles of the type $\{e'_1, e_2 + e_3 + e_4\}$. The two edges parallel to e'_1 are glued on two atomic surfaces, and we are left with the four sets of edges of the type $e_2 + e_3 + e_4$. But it is easy to see that these segments form the edges of a lattice of small octagons contained in planes parallel to \mathbf{E}_{\parallel} . We just add these octagons as our second step and we are done: the “completed” atomic surfaces have no longer any boundary.

In fact, this procedure is interesting because it changes nothing to the construction of the tiling: the new pieces are non transversal to \mathbf{E}_{\parallel} , so that a

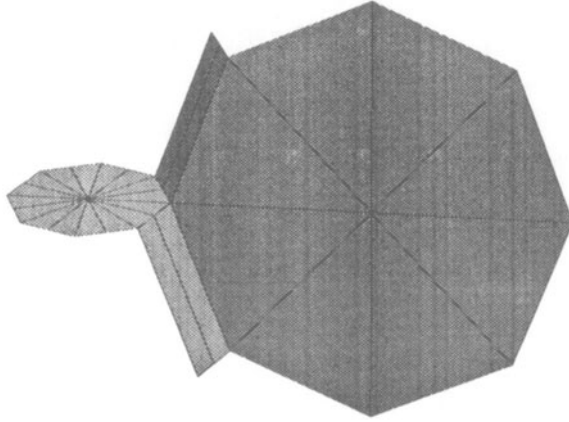


Fig. 26. — A (slightly metaphoric) description of the closure of the atomic surfaces of the octagonal tiling: the first step consists in gluing rectangles to the edges of the main octagon in \mathbf{E}_\perp ; the second step closes the surface by adding a small octagon contained in \mathbf{E}_\parallel . The main octagons in \mathbf{E}_\perp are disconnected from each others by the forbidden planes whose traces are drawn on the figure.

generic plane cut never intersect them. The geometry of the complete atomic surface is illustrated on Fig. 26.

Now, we are lucky, because the forbidden planes also intersect the completed atomic surfaces in a non-transversal way, namely along line segments. On Fig. 26, one can see that, first, the four forbidden planes of second kind intersect the original atomic surface (the large octagon) along the diagonals and then cross the small octagon also along the diagonals while, second, the four forbidden planes of the first kind divide in two the rectangles before crossing the small octagon. All eight planes intersect on the center of the small octagon which is located on the body center of the lattice (the center of large octagons being on the vertices of this lattice).

Thank to this highly non generic configuration, it is easy to discuss our question. Consider a cut intersecting the atomic surface of Fig. 26 inside the large octagon, and let us try to move this point: its trajectory defines a line on the atomic surface and it is quite obvious that it is impossible to make such a line between two large octagons without intersecting one of the forbidden

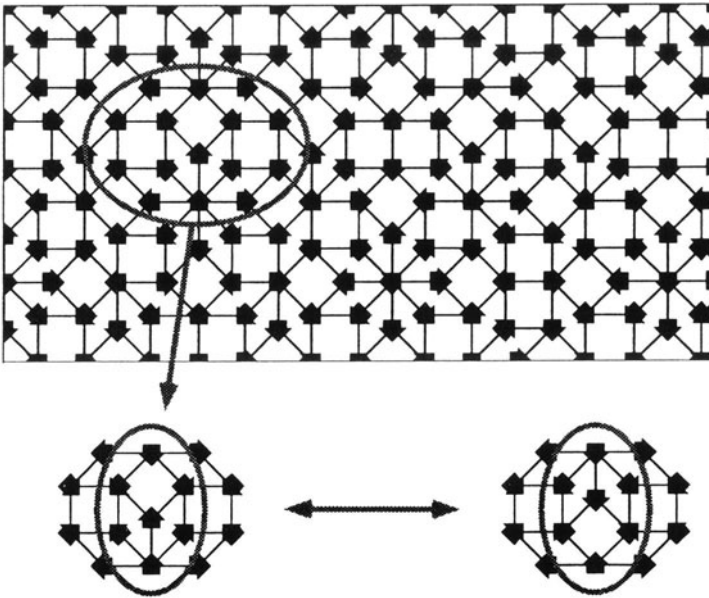


Fig. 27. — The vertex rules are only weak: it is possible to flip a hexagon while keeping a well-decorated tiling; however, such a flip does not open new possibilities besides the reverse flip.

planes of the first kind, whose traces surround completely the large octagon.

This confirms that the rules involving the forbidden planes of the first kind are strong ones (for regular tilings). But now consider the second family of forbidden planes: we see that their traces on the completed atomic surfaces build closed polygons made of four pairs of segments joining the center of a large octagon to one of its vertices, then to the center of the small octagon sharing this vertex. We see that a cut constrained not to exit of this polygon may wander from one large octagon to a neighbouring one, but cannot go further. Thus the matching rules for the generalised Ammann tilings of the second kind are only weak: given such a regular tiling, it is possible to flip some hexagons without violating the rule. Such a flip creates a new hexagon, but you cannot flip it without violating the rule: a cut compatible with the forbidden plane may only oscillate between two and only two atomic surfaces. This is illustrated on Fig. 27, where one can see that the characteristic feature of the “flippable” hexagons is that their two tips (right angles) bear the same trace of the large Ammann arrow (a square), which is not always the case for tips occupied by a pair of rhombi.

8. CONCLUSION

Let us first stress that nothing in the methods we have explained is limited to the two-dimensional case. For instance, the same ideas work for devising matching rules for the 3-dimensional (icosahedral) Penrose tilings (for which the method of forbidden planes was initially developed).

Now, one can draw several conclusions from this theory. The main one is that (at least in the author's mind . . .) the existence of matching rules is no longer mysterious. But this approach solves also a long-standing conjecture in this field, which was that matching rules are intrinsically linked with self-similarity. The case of generalised Ammann tilings shows that this is not the case: for almost all φ (along \mathcal{S}_1) and ψ (along \mathcal{S}_2), the quasiperiodic tilings do not have any self-similarity property. On the contrary, the real geometric key to matching rules seems to reside in non-transversality properties.

In the present framework, non-transversality is involved in three different ways. First, the direction of the cut must be non-transversal to a sufficient number of lattice subspaces. This corresponds to the existence of worms and is absolutely inherent to this approach. Second, we have described the cut through its intersections with fibers (here parallel to \mathbf{E}_\perp) which intersect non-transversally the forbidden planes, so that they are disconnected by these intersections. This allows a straightforward description of the homotopy classes of cuts. This context could perhaps be slightly relaxed: in situations where there does not exist a common fiber simultaneously non-transversal to all the forbidden planes, one could perhaps work with several fibers, each of them being non-transversal to a sufficient subset of forbidden planes.

The third way non-transversality is involved concerns the shape of the atomic surfaces: as we have seen, they must be bounded along the intersections of their carrier (here \mathbf{E}_\perp) with the forbidden planes. This is the second condition to get worms, and is also inherent to this approach. In view of the structure determination of quasicrystals (which amounts essentially to construct a set of atomic surfaces) this constraint is of primary importance. In fact, if you trust that matching rules have something to do with real quasicrystals, you can restrict your search for atomic surfaces to a limited class of polyhedra, which is of course an enormous restriction. Thus, besides its own geometrical interest, we may hope that this theory will help solving the structure of quasicrystals.

References

- [1] L. S. Levitov, *Commun. Math. Phys.* **119** (1988) 627.
- [2] A. Katz, *Commun. Math. Phys.* **118** (1988) 263.
- [3] F. Gähler, *Journal of Non-Crystalline Solids* **153 & 154** (1993) 160.
- [4] J. E. S. Socolar, *Commun. Math. Phys.* **129** (1990) 599.
- [5] R. Penrose, *Mathematical Intelligencer* **2** (1979) 32.
- [6] N. G. de Bruijn, *Nederl. Akad. Wetensch. Proc. Ser. A* **43** (1981) 39.
- [7] H. Bohr, *Acta Math.* **45** (1924) 29.
- [8] H. Bohr, *Acta Math.* **46** (1925) 101.
- [9] H. Bohr, *Acta Math.* **47** (1926) 237.
- [10] A. S. Besicovitch, *Almost periodic functions*, Cambridge University Press, Cambridge, (1932).
- [11] P. Bak, *Scripta Met.* **20** (1986) 1199.
- [12] A. Janner and T. Janssen, *Phys. Rev. B* **15** (1977) 643.
- [13] P. M. de Wolff, *Acta Cryst.* **A30** (1974) 777.
- [14] A. Katz and M. Duneau, *Journal de Physique* **47** (1986) 181.
- [15] C. Oguey, M. Duneau and A. Katz, *Commun. Math. Phys.* **118** (1988) 99.
- [16] P. Kramer, *J. Math. Phys.* **29** (1988) 516.
- [17] B. Grünbaum and G. C. Shephard, *Tilings and Patterns*, W. H. Freeman, San Francisco, (1987)
- [18] Beenker F. P. M., Algebraic theory of non-periodic tilings by two simple building blocks: a square and a rhombus (Eindhoven, TH-Report 82-WSK-04, 1982).
- [19] A. Katz and D. Gratias, in *Lectures on Quasicrystals (Aussois 1994)*, edited by F. Hippert and D. Gratias, Les Editions de Physique, Paris (1994).
- [20] L. Danzer, *Discrete Math.* **76** (1989) 1.
- [21] P. Stampfli, *Helv. Phys. Acta* **59** (1986) 1260.
- [22] E. Zobetz, *Acta Cryst.* **A48** (1992) 328.
- [23] J. E. S. Socolar, *Phys. Rev. B* **39** (1989) 10519.
- [24] R. Klitzing, M. Schlottmann and M. Baake, *Int. J. Mod. Phys. B* **7** (1993) 1455.
- [25] R. Klitzing and M. Baake, *Journal de Physique I* **4** (1994) 893.
- [26] T. Kupke and H. R. Trebin, *Journal de Physique I* **3** (1993) 564.
- [27] R. Ammann, B. Grünbaum and G. C. Shephard, *Discrete Comput. Geom.* **8** (1992) 1.
- [28] P. A. Kalugin, *Europhys. Lett.* **9** (1989) 545.